

WIYN¹Open Cluster Study 5. Lithium Depletion and Metallicity in G and K Dwarfs of the Open Cluster M35.

David Barrado y Navascués²

*Max-Planck-Institut für Astronomie. Königstuhl 17, Heidelberg, D-69117 Germany.
barrado@pollux.ft.uam.es*

Constantine P. Deliyannis

Astronomy Department, Indiana University, Swain Hall West 319, 727 E. 3rd Street, Bloomington, IN 47405-7105, USA. con@athena.astro.indiana.edu

John R. Stauffer³

*Harvard-Smithsonian Center for Astrophysics, 60 Garden St., Cambridge, MA 02138, USA.
jstauffer@cfa.harvard.edu*

ABSTRACT

We present an analysis of high quality spectra of members of the young cluster M35. By using a multi-fiber spectrograph, we are able to collect high signal-to-noise, high resolution spectra of a sample of photometric candidate members. Accurate radial velocities are used to establish the membership status and rotational velocities are measured using cross-correlation. We also derive the metal content of the cluster, $[Fe/H]_{M35} = -0.21 \pm 0.10$, based on spectral synthesis. Finally, we derive the lithium abundances of the *bona fide* cluster members and compare the results with members of other clusters. For example, M35 shows a smaller range in both rotation rates and lithium abundances as compared to the Pleiades. We discuss possible roles of various parameters. Our high quality M35 database of lithium abundances and rotational velocities are perfectly suited to be used as a laboratory to test theoretical models dealing with the lithium depletion phenomenon. We discuss the role of stellar inhomogeneities and rotation on the lithium depletion phenomenon.

Subject headings: stars: abundances – stars: late-type – open clusters and associations: M35, NGC 2168

1. Introduction

Late spectral type stars share a series of characteristics which make them extremely interest-

²Present address: Departamento de Física Teórica, C-XI. Universidad Autónoma de Madrid, Cantoblanco, E-28049 Madrid, Spain

³Present address: IPAC, California Institute of Technology, Pasadena, CA 91125, USA

¹The WIYN telescope is maintained and operated by a consortium whose member institutions are University of Wisconsin, Indiana University, Yale University, and the National Optical Astronomy Observatories.

ing objects. Among other parameters, these properties usually depend on the age and the stellar mass. These stars have activity which is analog to the one present on the Sun, arising from the stellar corona, the chromosphere and the photosphere. This activity is produced as a consequence of the interaction between differential rotation and magnetic fields, the so-called stellar dynamo (Parker 1955). Rotation itself is a very important characteristic, with a dependence on mass and age not fully understood. The understanding of these properties require to locate them in an evolution-

ary scenario. This is done by studying members of open clusters of different ages and metallicities, so we can determine which is the particular role of age, stellar mass and chemical composition.

Lithium is a chemical element which can be used as a probe to the internal structure, since convection transports the material downward to layers hot enough to destroy lithium by interactions with protons. Due to this, its surface abundance depends strongly on age for a given mass during the pre-Main Sequence (pre-MS) phase. And, because of increasing depth of the convective envelope when moving to less massive stars, the lithium abundance also depends on mass. (or stars of spectral type later than F8, at a given age, more massive stars have higher Li.) After the pre-MS phase, additional mixing mechanisms are needed, in order to explain the lithium abundance of FGK spectral type members of clusters of different ages. For recent reviews, see Deliyannis (2000) and Jeffries (2000). In particular, Deliyannis (2000) stresses the stellar mass as the first parameter controlling Li depletion, and age the second parameter. Additional parameters might be composition, and initial angular momentum. There have been reported a significant amount of studies on the evolution of lithium with age and the dependence on mass. Updated reviews on the lithium phenomenon, from the theoretical and observational point of views, can be found in Vauclair (2000) and Martín (2000), respectively. Very well known open clusters such as the Hyades, Praesepe, Coma, M67 and Alpha Per have been exhaustively investigated, as well as other not so famous, and the behavior of lithium in their members analyzed. The Pleiades has played a *prima donna* role in these investigations. Duncan & Jones (1983) showed that G Pleiades stars have significant lithium abundances differences. Butler et al. (1987) reported a scatter for rapid rotators of K spectral type, confirmed by García López et al. (1991a,b), and Soderblom et al. (1993a). García López, Rebolo, & Martín (1994) added more data to the sample and established that the relation between fast rotators and high lithium abundances broke down for stars at $T_{eff} < 4500$ K. Jones et al. (1996) examined the late K and Russell (1996), Stuik et al. (1997), Jeffries (1999), King, Krishnapurthi & Pinsonneault (2000) and Barrado y Navascués et al. (2000) have recently dealt with

the origin of the lithium spread in K Pleiades stars, without solving completely the puzzle.

The M35 cluster (NGC2168) is, allegedly, co-eval to the Pleiades, since their turn-off is located in the same position in the color-magnitude diagram (Vidal 1973). Due to several properties, it has a promising future as a target for this type of studies. Although it is moderately far away $-(m-M)_0 = 9.7$ magnitudes, compared with $(m-M)_0 = 5.36$ in the case of the Pleiades, Robichon et al. (1999)–, it has a clear advantage over other associations: its richness. It is one of the richest nearby young clusters, with a total mass estimated between 1600 and 3200 M_\odot (Leonard & Merritt 1989). Membership of those (few) stars hotter than about 5700 K can be checked against the excellent proper motion membership study of McNamara and Sekigushi (1985). In addition, several optical surveys have been recently conducted, producing long lists of candidate members (Sung & Bessell 1999; von Hippel 2000; Sarrazine et al. 2000). The recent study by Sung & Bessell (1999) yields $(m-M)_0 = 9.60 \pm 0.10$, $E(B-V) = 0.255 \pm 0.024$ and an age of 200^{+200}_{-100} Myr, somewhat older than the turn-off age of the Pleiades, 80 Myr. Similar results have been derived by Sarrazine et al. (2000), including $(m-M) = 10.16 \pm 0.01$, $E(B-V) = 0.198 \pm 0.008$, and an age of 160 ± 40 Myr.

For some time now, we have been studying exhaustively this cluster, tackling problems such as the mass function of the cluster (Barrado y Navascués et al. 1999, 2000a), rotational periods, and multicolor photometric surveys (Barrado y Navascués et al. 2000a). Moreover, since the cluster covers less than 1 sq.deg., it is a perfect candidate for multi-object spectroscopy. We have taken advantage of the WIYN/HYDRA multi-fiber spectrograph and observed a sample of M35 candidate members, with the goal of identifying *bona fide* members, determining the pattern of lithium depletion and rotation for them, and establishing the connection between these two last properties (rotation and lithium). We present the data in Section 2, whereas the analysis and comparison with open clusters, including the Pleiades, are discussed in Section 3. A summary and the main conclusion can be found in Section 4.

2. The data

2.1. M35 observations and data reduction

We selected our initial sample of M35 photometric candidate from Barrado y Navascués et al. (2000a). In that paper, we produced a list of cluster candidates based on their location in a V, I_c and I_c, R_c color-magnitude diagrams. Our targets have colors and magnitudes in the ranges $V=14.5-17.5$ and $(V-I)_c=0.85-1.55$. Figure 1 displays the location in a color-magnitude diagram of our target stars. In total, we observed 76 candidate members of the cluster. Table 1 lists the names and positions of these stars, as well as the photometry (our data from Barrado y Navascués et al 2000a and a compilation of data from Sung & Bessell 1999). The last column in Table 1 indicates the membership status of these candidates (see Section 3.1).

Our candidate members were observed spectroscopically using WIYN/HYDRA, a multifiber spectrograph, capable of observing 97 targets simultaneously. We took 6 individual exposures of ~ 2 hours each, over 2 different nights.

The reduction was carried out with the IRAF⁴ environment, using standard procedures (bias subtraction, flat-fielding, extraction of the individual spectra and wavelength calibration). IRAF contains a specific package which performs optimally all these functions in a standardized way, denominated "dohydra". The final free spectral range is 6440-6850 Å, with a resolution of $R \sim 20\,000$, as measured in the comparison lamp spectra (2 pixels). Since we collected spectra in two consecutive nights, and within each night the observations were split in individual exposures two hours long each, we processed each individual set of spectra in a complete independent way. Once the exposure was reduced and the individual spectra were extracted for each star, we combined all the spectra corresponding to the same star using a median filter, in order to remove remaining cosmic rays. The signal-to-noise ratios range from 40 per pixel for our faintest objects, to 160 in the case of the brightest. This is a remarkable feat for stars which are at $(m-M)=10.4$ magnitudes. Some examples

of spectra of our sample of M35 candidates are shown in Figure 2. The effective temperature decreases upward. Note the obvious change of the $H\alpha$ equivalent width and profile, and the presence of the lithium doublet at $Li\,I\,6708\text{\AA}$.

2.2. Data from other clusters.

In the next sections we will analyze the data we have derived for M35 candidate members. We will also compare our data with data collected from a number of open clusters, namely the Pleiades, NGC2516, M34 –NGC1039–, NGC6475, Ursa Majoris moving group –UMaG– and the Hyades. The turn-off ages of these clusters lie in the ranges 70–100, 120–150, 200, 220, 300 and 600–800 Myr, respectively. At the present time, our group has estimated the ages of the open clusters IC2391 (Barrado y Navascués, Stauffer & Patten 1999), Alpha Per (Stauffer et al. 1999), and the Pleiades (Stauffer, Schultz, & Kirkpatrick 1998), based on the lithium depletion boundary technique (LDB) in very low mass members of each cluster. These LDB ages are ~ 50 % older than the turn-off ages. However, they agree with turn-off ages computed with a moderate amount of core overshooting (Ventura et al. 1998). In fact, Stauffer & Barrado y Navascués (1999) have been able to define a new age scale for young open clusters based on the lithium dating technique, in opposition to the Upper Main Sequence age scale, such as that from Mermilliod (1981). Note that in the new LDB age scale, the Pleiades is 125 ± 5 Myr. Although there are now very deep photometry of M35, reaching the lithium depletion boundary of the cluster (Barrado y Navascués et al. 1999, 2000a), the distance modulus of the cluster is so large that it poses an extraordinary challenge to detect lithium at the bottom of its Main Sequence even with the largest telescopes and a significant amount of observing time. Regardless of the age scale we use, the conclusions of this study remain the same, providing we use ages in the same scale for each cluster. Therefore, we will work with the turn-off age scale, keeping in mind that the real ages may be a 50 % older.

The data for these clusters we are going to compare come from several sources. In the case of the Pleiades, photometry, rotation, activity, and lithium equivalent widths come from Soderblom et al. (1993a), García López, Rebolo, & Martín

⁴IRAF is distributed by National Optical Astronomy Observatories, which is operated by the Association of Universities for Research in Astronomy, Inc., under contract to the National Science Foundation, USA

(1994), Jones et al. (1996) and Jeffries (1999). Additional photometric data were selected from Johnson & Mitchell (1958), Stauffer (1982, 1984), and Stauffer & Hartmann (1987). NGC2516 data come from Jeffries, James, & Thurston (1998). Jones et al. (1997) is the source of M34 data, whereas James & Jeffries (1997) provides the information for NGC6475. Data for UMaG were collected by Boesgaard et al. (1988) and Soderblom et al. (1993c). Finally, Hyades data were selected from a number of sources, including Duncan & Jones (1983), Boesgaard & Tripicco (1986), Rebolo & Beckman (1988), Soderblom et al. (1990), Thorburn et al. (1993), Barrado y Navascués & Stauffer (1996). We have to point out that in some cases, these databases only provide the $(B-V)$ or $(V-I)_k$ color indices, whereas our M35 sample was observed in the V, I_c filters. In general, we look for additional data in these last two bands, losing some stars which do not have this type of data. In some cases, we only could find data in the Kron system, instead the Cousins system. Then, the $(V-I)_k$ color was transformed into $(V-I)_c$ color using Bessell & Weis (1987) transformation. However, for other comparisons, we preferred to keep all the original sample (such as in some comparisons between M35 and the Pleiades). In this case, we converted those $(B-V)$ Pleiades values into $(V-I)_c$ colors using an average relation between these colors which was computed using Pleiades stars observed in both colors. This transformation introduces a bias, due to the inhomogeneous reddening for some Pleiades stars (Soderblom 1993b). We emphasize that all the data for these seven clusters were treated in an homogeneous way (for instance, the derived lithium abundances).

3. Analysis

3.1. Radial velocities and membership

Our spectral resolution ($R \sim 20,000$) allows us to compute radial velocities to an accuracy of ~ 1 km/s. This was achieved by measuring the positions of strong lines (from iron and calcium) on the spectra and deriving the shifts respect their rest wavelengths. We also performed cross-correlation against M35 candidate members. HYDRA is a bench spectrograph and, therefore, the wavelength calibration is very precise (that is, it always yields the same value). In any case, even if there is any

shift having other origin than the relative velocity of the M35 candidates and Earth, this unlikely shift should be the same for all stars in our sample, since a particular exposure for a star was obtained simultaneous to the rest of candidates. Since we have several exposures which were taken during two consecutive nights, we have measured radial velocities in each of them. Therefore, we have 11 data-points for each M35 candidate member.

Based on the radial velocity information, we have classified our M35 candidate members in three different categories:

- Probable members, single stars. These stars do not present variability on the radial velocity (at least in the time scale of our series of observations, two days) and the measured values are well within the average radial velocity of the cluster ($\langle RV \rangle_{M35} = -8.0 \pm 1.5$ km/s). There are 39 objects in this group. Average radial velocities and dispersions are listed in column #2 of Table 2 for these stars.
- Possible members, spectroscopic binaries. This group includes all the candidates with variable radial velocity. Some of them show lines arising from both components of the system. Since we have obtained only a handful of spectra per star, we are not able to estimate the radial velocity of the baricenter and, therefore, to determine their membership status. There are 13 objects in this category, including 3 SB2 binaries
- Probable non-member. Those stars whose radial velocity is constant and different to the cluster average have been classified as non-members based on this criterion. Moreover, the majority of these stars have a remarkable weak Li 16708Å doublet. Most field stars are likely to be older than the very young M35, and are thus likely to have depleted their Li, consistent with our findings.

Note that we only have used lithium as a membership criterion to confirm the classification as a non-member of stars falling in this group. Figure 1 depicts all the stars in our sample, probable members, possible SB members and non-members, as solid circles, empty circles and crosses, respectively. Since our goal is to study the proper

ties of dG–dK members of the M35 cluster (rotational velocities, metallicity, activity and lithium abundances), we do not consider further the non-member. See Barrado y Navascués et al. (2000a) for more information about them. We defer the discussion about the possible binaries of M35 to a forthcoming paper, which will analyze the lithium abundance and photometric properties of the components in the same fashion as Barrado y Navascués & Stauffer (1996) and Barrado y Navascués et al. (1997b), where we presented an exhaustive and comprehensive analysis of long period and tidally locked binaries belonging to the Hyades and M67 open clusters. For the special role that short period binaries play in testing models of lithium depletion caused by rotationally induced mixing, see discussion in Deliyannis (1990); for related discoveries of high-Li short binaries, see, a) in the Hyades (Thorburn et al. 1993), b) in M67 (Deliyannis et al. 1994), and c) in the field and metal-poor stars (Ryan and Deliyannis 1995). For a general description from the phenomenological point of view of the role of binarity on the lithium depletion phenomenon, see Barrado y Navascués (1998).

3.2. Rotational velocities

Rotational velocities were derived by cross-correlation technique. First, we selected one spectrum with very narrow lines, and spinned it up using rotational broadening functions with rotational velocities from 10 km/s to 90 km/s, with increments of 10 km/s. These artificially broadened spectra were cross-correlated with the candidate members, using the spectral range 6600–6730 Å. The $v \sin i$ values are listed in the last column of Table 2.

Figure 3a depicts our measured rotational velocity against the dereddened $(V-I)_c$ color index for all the probable members of M35. Solid circles represent actual measurements, whereas solid triangles correspond to upper limits. As a comparison, we have included data from the Pleiades, which were selected from Soderblom et al. (1993a). This sample appears as crosses in the figure. Despite of its youth, M35 lacks rapid rotators in this color range. Only a handful of the warmer stars in the sample have projected rotational velocities well above the detection limit. Their velocity ranges between 20 and 30 km/s.

Only one star in the cooler end (M35-5376) has a high rotational velocity. (In fact, the largest among our sample of probable members of the cluster.) However, stars belonging to the Pleiades open cluster show a very different pattern in their distribution of rotational velocities. A significant amount of them have values larger than 50 km/s, even reaching 130–140 km/s in two cases. Since M35 and the Pleiades have, allegedly, the same age, this situation defies, till certain extent, our understanding of the age-rotation connection. It should be taken into account that the Pleiades $(V-I)_c$ values were derived from $(B-V)$ colors. To avoid any possible bias introduced by this process, we have re-plotted the data in Figure 3b using measured $(V-I)_k$ colors for Pleiades stars and transforming them into $(V-I)_c$. Some of these stars have disappeared from scene, due to the lack of adequate photometry. More important, some of these Pleiades stars have been shifted red-wards, and they lie now on top of the M35 cool rapid rotator. The lack of concordance between $(B-V)$ and $(V-I)$ photometry has been noticed by King, Krishnamurthi & Pinsonneault (2000), who pointed out that it could be due to errors in one passband or to increased red flux from stellar spots. In fact, they found, in their words “... strong evidence that our Teff values ... are affected by activity level.” But the conclusion still holds, the Pleiades has a significant amount of fast rotators which are not present in M35. Other parameters might be working, such as a difference in metallicity (see next subsection) and/or a different initial angular momentum distribution (it would have been more uniform in M35). An additional piece of information can be extracted from the comparison between M35 and NGC2516 data, shown in Figure 3c. The similitude of both distributions is remarkable, an understandable phenomenon if, as pointed out by Sung & Bessel (1999), M35 is 200^{+200}_{-100} Myr, and therefore closer in age to NGC2516 than to the Pleiades.

3.3. The metallicity of M35

The lithium depletion depends, among other parameters, on age, rotation and metallicity (see recent reviews by Balachandran 1995; Pinsonneault 1997; Martín 2000). Therefore, in order to interpret correctly our observations, we have to take into account the metal content, specially if

we intend to infer conclusions by comparison with other clusters. To our knowledge, there is no previous spectroscopic study of the metallicity of this cluster. Sung & Bessell (1999), based on photometric data (UBVI filters), estimated $[\text{Fe}/\text{H}]_{\text{M35}} = -0.3$. Gratton (2000), using DDO photometry, estimated $[\text{Fe}/\text{H}]_{\text{M35}} = -0.28$. We have obtained an independent estimate of the M35 metallicity based on spectral synthesis. We have used the MOOG spectral synthesis program (Sneden 1973) and Kurucz (1992) model atmospheres. In all cases, we used a gravity of $\log g = 4.5$. The gf-values were derived by Balachandran (private communication), via spectral synthesis of solar equivalent widths (Kurucz et al. 1984). We applied these data to a subsample of our *bona fide* M35 single probable members. This group includes the 9 brightest-warmest stars, with the highest S/N. The spectrum of some of these stars can be found in Figure 2.

We measured the equivalent widths of several iron lines present in the observed spectral range (about 10 per star, see Table 3). We acknowledge that the number of lines is small, due to the short free spectral range, and all of them belong to the ion Fe I. These facts introduce uncertainties in the final estimate. The $[\text{Fe}/\text{H}]$ value was derived in two different ways: (i) We used the effective temperature evaluated from the photometry (temperature scale from Bessel 1979, with values derived from $(V-I)_c$, listed in Table 1). A model atmosphere with this temperature was introduced in MOOG as input in order to derive the iron abundance for each line. We list the average value in columns #2 and #3 of Table 4. (ii) We adjusted the effective temperature (spectroscopic temperatures) with MOOG in order to obtain the similar values of $[\text{Fe}/\text{H}]$ for all lines at different excitation potentials. The results, as well as their standard deviations, are listed in columns #4 and #5 of Table 4.

Figure 4 shows both sets of results (data derived using spectroscopic and photometric temperatures appear as solid and empty circles). The average values in both cases are very similar, within the uncertainties. We have adopted a metallicity for the M35 cluster of $[\text{Fe}/\text{H}]_{\text{M35}} = -0.21 \pm 0.10$ dex, corresponding to the average value of our individual metallicities. In order to compare with the Pleiades open cluster, we proceeded

in the same way with several Pleiades members of the same color range (spectra kindly provided by D. Soderblom). In this case, the result is $[\text{Fe}/\text{H}]_{\text{Pleiades}} = +0.01$ dex. This value can be compared with those results for the Pleiades by Cayrel, Cayrel de Strobel, & Campbell (1988), $+0.13$ dex; Boesgaard & Friel (1990), -0.034 ± 0.024 dex; Gratton (2000), -0.03 ± 0.06 dex; and King et al. (2000), $+0.06 \pm 0.06$ dex. Figure 4 also shows our two average metallicities for M35 and the Pleiades (solid and dashed lines, respectively). We conclude that M35 is slightly metal-poor compared with the Pleiades.

3.4. The Age of M35

Vidal (1973) estimated, based on the turn-off of the Pleiades and M35 massive stars, that both clusters have the same age. However, this comparison was made using photographic data. Deep, accurate CCD photometry for M35 has not been available until very recently (Barrado y Navascués et al. 1999; Sung & Bessel 1999; von Hippel et al. 2000; Barrado y Navascués et al. 2000a). This wealth of new data allows an accurate age determination. Sung & Bessell (1999), using isochrone fitting in multiple color-magnitude diagrams, have derived an age of 200^{+200}_{-100} Myr, significantly older than the Pleiades standard age of 80 Myr. The isochrone fittings of the red giant probable member and the two red giants possible members give 125 and 200 Myr, respectively. The same qualitative results have been obtained by von Hippel et al. (2000) fitting the MS of the cluster. Moreover, Sarrazine et al. (2000) have estimated, using several color-magnitude and color-color diagrams in the UBVRI bands, that the age is 160 ± 40 Myr. As comparison, they applied the same technique to the Pleiades and derived a turn-off age of 80 ± 20 Myr. Mysore (1999) analyzed a sequence of M35 V band images, identified a set of probable M35 members, and searched for photometric variability due to starspots among the G and K dwarf cluster members. Despite being sensitive to variability sufficient to easily identify stars like the rapidly rotating K dwarfs in the Pleiades (which have typical light curve amplitudes in V of about 0.1 mag), she found no certain M35 variables. She concluded from this that M35 is likely to be significantly older than the Pleiades.

These age ranges fully agree with our own find-

ings concerning the distribution of rotational velocities and, as we will see, the lithium depletion. Therefore, we will assume that M35 is a 175 Myr old cluster, the average age of the three M35 red giants.

3.5. Lithium abundances

3.5.1. The lithium equivalent widths

We have measured the lithium Li I 16707.8Å equivalent widths $-W(\text{Li I})-$ for all our M35 candidates. Due to our spectral resolution, the high lithium abundances and the rotation velocities, the lithium feature is blended with Fe I 16707.4Å. Therefore, we removed this small contribution using an empirical relation between color and $W(\text{Fe I})$ derived by Soderblom et al. (1993a). We list the blended and deblended equivalent widths $W(\text{Li+Fe})$ and $W(\text{Li})$ in columns #3 and #4 of Table 2. Before analyzing the pattern of lithium depletion in M35, let's examine first how the lithium equivalent widths depend on the color, dependence depicted in Figure 5. Solid circles and crosses represent M35 probable members and Pleiades data from Soderblom et al. (1993a), respectively. The $(V-I)_c$ color indices used in panel a were derived from $(B-V)$, whereas those shown in panel b come from $(V-I)_k$ values (see section 2.2). It is easy to appreciate the scatter present in the Pleiades data. For a discussion about the origin of this spread, see Soderblom et al. (1993a), King, Krishnamurthi & Pinsonneault (2000), Barrado y Navascués et al. (2000b), and Section 3.5.3. This scatter is more conspicuous for stars redder than $(V-I)_{c,0}=0.8$. On the other hand, M35 stars in the range $0.6 < (V-I)_{c,0} < 1.0$ have, within the errors, a tighter relation between $W(\text{Li I})$ and the color index. However, as it happens in Pleiades stars, there is an important scatter for cooler M35 stars. Moreover, on average, M35 stars show a smaller lithium equivalent widths for a given color, when compared with the Pleiades. If both clusters have the same age, this situation is difficult to understand (this also was the case of rotational velocities, with Pleiades stars rotating faster than equivalent M35 stars). Why do M35 stars have smaller $W(\text{Li I})$ than their Pleiades counterparts? Why is the relation better defined in M35? What is the origin of the scatter around $(V-I)_{c,0} \sim 1.2$? In the next subsections we will try to shed some

light over these problems.

3.5.2. The $T_{\text{eff}}-A(\text{Li})$ plane

We have derived lithium abundances for all stars discussed here using the curves of growth computed by Soderblom et al. (1993a). After measuring the lithium equivalent widths (or gathering them from the literature in the case of the other open clusters, see Section 2.2), the following step was used to estimate effective temperatures. Since temperature scales based on $(B-V)$ colors are more sensitive to metallicity than those based on $(V-I)$, and our clusters have different metal content ($[\text{Fe}/\text{H}]_{\text{M35}}=-0.21$, $[\text{Fe}/\text{H}]_{\text{Pleiades}}=+0.01$ –both from this paper, see section 3.4–, $[\text{Fe}/\text{H}]_{\text{NGC2516}}=-0.32$ –Jeffries et al. (1997)–, $[\text{Fe}/\text{H}]_{\text{M34}}=-0.29$ –Gratton 2000–, $[\text{Fe}/\text{H}]_{\text{NGC6475}}=+0.11$ –James & Jeffries 1997–, $[\text{Fe}/\text{H}]_{\text{UMaG}}=-0.079$ or -0.085 –Boesgaard et al. 1988 and Boesgaard & Friel 1990, respectively–, $[\text{Fe}/\text{H}]_{\text{Hyades}}=+0.16$, or $+0.127$, or $+0.13$ –Cayrel, Cayrel de Strobel, Campbell 1988; Boesgaard & Friel 1990; and Gratton 2000, respectively–), we derived effective temperatures from $(V-I)_c$ colors, after Bessell (1979) temperature scale. The effective temperature values are listed in columns #6 and #8 of Table 2. In the first case, the temperature was computed using our values of $(V-I)_c$ (Barrado y Navascués et al. 2000a), whereas in the second case we used the color indices selected from Sung & Bessell (1999). These two sets of effective temperatures and the lithium equivalent widths were used to derived the lithium abundances listed in columns #7 and #9 of the same table. As can be seen, there is not relevant differences in both cases. (i.e., the scatter introduced on the final lithium abundances by differences in the photometry of individual M35 stars is quite small.) From now on, we will used the effective temperatures and lithium abundances derived with our photometry. Errors in the computed abundances were estimated taking into account the uncertainties in effective temperatures and lithium equivalent widths.

Figures 6a and 6b are like Figures 5a and 5b, but in this case we depict the abundance $-A(\text{Li})$ in the customary scale where $A(\text{Li})=12+\log(\text{Li/H})-$ against the effective temperature. Note that the temperatures corresponding to Pleiades stars which are shown in Figure 6a come directly from

Table 1 of Soderblom et al. (1993a) and, therefore, they were computed from (B-V) colors. There are three features in these figures which are worth discussing:

1.- Independently of the origin of the Pleiades temperatures, it seems clear that, for a given spectral type, M35 stars have depleted more lithium than similar Pleiades stars. This phenomenon is more conspicuous in the range 6000-5500 K, where the Pleiades show abundances close to the cosmic value $-A(Li)_{cosmic}=3.2$, Rebolo (1989), Anders & Grevesse (1989); Martín et al. (1994)–, whereas M35 members have abundances below $A(Li)=3.0$ dex. If indeed the Pleiades and M35 have the same age, this situation arises some concerns on our understanding of the processes taking place during the lithium depletion in pre-MS stars and its relation with age. The distribution of rotational velocities is similar for both clusters in this temperature range, and a rotational effect cannot be responsible of the differences in lithium abundances. The difference in metallicity cannot also be called upon as the main actor, since the difference is small and it would act in the opposite direction: the bottom of the convective envelope would be closer to the surface in the case of M35, making more difficult the lithium depletion.

2.- Pleiades stars in the range 5300-5000 K have a very relevant lithium spread, related to rotation and activity (Butler et al. 1987; Soderblom et al. 1993a; García López, Rebolo, & Martín 1994), larger than 1 dex. This scatter does not appear in the case of M35 members. However, this situation does not prove the lack of connection between lithium depletion and rotation/activity, since these M35 members are very slow rotators. That is, there is no slow rotator with high abundance and *vice versa*, a fact which either would contradict the relation between lithium depletion and rotation, or would indicate that the rotational history is playing an important role (in opposition to a sharp connection rotation–lithium for a given age). See section 3.5.3 for an additional discussion about the lithium spread.

3.- Stars at lower temperature (Teff~4500 K) do show a large spread ($\Delta Li > 1.0$ dex). The spread is quite apparent if the spectra of these stars are compared (see Figure 7a,b). This spread is marginally related to rotation, but unfortunately our sample only contains one cool fast rotator

and it is safer not to derive any conclusion at the present stage. Only additional data can establish the origin of this spread and its relation with rotation and activity.

There are four M35 probable members with only upper limits to their lithium abundances. Three of them are quiet cool, and their low abundances, below $A(Li)=0$ dex, can be explained by the dependence of the lithium depletion on mass, as happens in slightly cooler Pleiades stars. However, one among these stars, #5190, is warmer and its behavior clearly departs from that characteristic of similar M35 members at the same temperature. This is probably an indication of non-membership. However, since we only used radial velocities as membership criterion, we have left this star in our sample of members of the M35 cluster.

3.5.3. The connection lithium-rotation-activity

During the last decade, much has been discussed about the nature of the lithium abundance spread in Pleiades early K dwarfs. From the observational point of view, there are several pieces of evidence which support the fact that the derived abundances are real, the spread is real, and it is connected with the stellar rotation rate. Butler et al. (1987) were the first to notice the spread and its relation with rotation, followed by García López et al. (1991a,b). Soderblom et al. (1993a) carried out a systematic analysis of the lithium spread and its relation with rotation and activity, using different indicators such as H α and the Ca II infrared triplet. They also considered the possible effect of stellar spots on the apparent lithium equivalent widths and the derived abundances, concluding that the spread was real, and that for a given color, those stars rotating faster had the largest lithium abundances and chromospheric activity. Jones et al. (1996) provided additional data, including cooler K spectral type stars. They confirmed the spread for early K and the break down of the relation for the fainter objects, noticed by García López et al. (1994).

However, other studies, either from the observational or the theoretical point of views, have challenged these results and their interpretation. Houdebine & Doyle (1995) computed a grid of model atmospheres for M dwarfs in non local thermodynamical equilibrium, showing that very high

chromospheric activity levels could modify the strength of Li I 6708Å. Russell (1996) found that derived abundances for several Pleiades stars using Li I 6103Å are different than those computed with Li I 6708Å. The lithium spread disappeared with the former abundances. He interpreted the situation as an indication of the effect of chromospheric activity on the Li I line, in agreement with the results of Houdebine & Doyle (1995), although Martín (1997) has pointed out the difficulty of deriving abundances using Li I 6103Å due to the presence of much stronger nearby lines and Stuik et al. (1997) affirmed that Li I 6708Å and K I 7699Å are not very sensitive to the presence of a chromosphere. They argued that the potassium feature can be used as a proxy to understand the formation of the lithium line without the effect of the abundance spread. Note that the K I 7699Å equivalent width does not depend on age, since potassium is not depleted in the stellar interior, in opposition to what happens to lithium. However, they could not establish if the magnetic activity can affect the K I 7699Å in Pleiades stars. In the same line, Jeffries (1999), by monitoring several Pleiades stars, concluded that it is still unsafe to attribute the spread to real abundance differences, and King, Krishnamurthi & Pinsonneault (2000) presented some additional evidences that the Pleiades lithium dispersion is partially due to stellar atmosphere effect. Moreover, they found a strong correlation between stellar activity and lithium abundances (see also Fernandez-Figueroa et al. 1993), but the relation between rotation and lithium abundance is not one-to-one, making unlikely that the reason of the lithium spread is rotation *per se*. Our own simulations (Barrado y Navascués et al. 2000b) indicate that stellar inhomogeneities (spots and active regions) could, indeed, introduce part of the lithium scatter, due to the combined effect of the inhomogeneities on the observed color (a star would appear to be cooler and less massive than it really is) and the equivalent widths (the observed lithium equivalent widths) would be increased in a significant amount, an effect noticed by Giampapa (1984). As shown by Barrado y Navascués et al. (2000b), the presence on the surface of stellar inhomogeneities can change in a significant way the observed colors and lithium equivalent widths, if the activity rates are very high (and, with them,

the filling factor or stellar spots and active regions). Doppler imaging of active Pleiades stars shows that they are, indeed, covered with huge polar spots (Stout-Batalha & Vogt 1999) of presumably long life span. The observed relation between lithium and rotation could be due, to some extent, to the link between rotation and activity. This situation does not mean that there are not genuine differences in the lithium abundances for stars of the same age and masses, and that these differences are related to the rotation and the rotational history of the star, as proposed by Deliyannis (1990), Deliyannis et al. (1990) and Pinsonneault, Deliyannis & Demarque (1991, 1992a,b). In fact, Barrado y Navascués et al. (2000b) have shown that under realistic conditions (when the filling factor of spots is less than 0.30), only part of the lithium spread can be attributed to surface inhomogeneities. Moreover, it has been shown that tidally locked binary systems (TLBS) in the Hyades and M67 have larger abundances than similar non-TLBS or single stars (Thorburn et al. 1993; Deliyannis et al. 1994; Ryan & Deliyannis 1995; Barrado y Navascués & Stauffer 1986; Barrado y Navascués et al. 1997b). Since most of the rotational periods of these Hyades and M67 TLBS are larger than any Pleiades star, the activity and the spot filling factor can not be invoked to explain these differences in abundances, which seem to be real. The same situation holds for chromospherically active binaries of different ages and evolutionary stages (Fernandez-Figueroa et al. 1993; Barrado y Navascués 1996, 1997; Barrado y Navascués et al. 1994, 1997a, and 1998). Therefore, the real lithium abundance differences due to rotation *per se* would be smaller than the values normally accepted. In this scenario, Pleiades rapid rotators would lose most of their angular momentum before they reach the M35 age, reducing their stellar activity. Therefore, the filling factor of stellar inhomogeneities would be reduced considerably, and the observed photometry and equivalent width of the star would be modify accordingly (the star would be moved blue-ward in the color magnitude diagram and Teff–lithium plane, due to the lack of cool spots). At this point, most of the lithium scatter would have disappeared. The remaining spread would be due to the real effect of rotation on the lithium depletion.

Figure 6 shows clearly that M35, an open clus-

ter significantly older than the Pleiades (Section 3.4), does not have a large scatter for early K stars. If the observed Pleiades scatter is due to real abundance differences and the Pleiades cluster represents the situation of M35 when it was 70-100 Myr old, it should be explained how the lithium spread has disappeared in these tens of million years. That is, all Pleiades stars for a given mass will have to deplete their lithium in a specific amount (more for those with the larger abundance) so they will end up with the same abundance once they reach M35 age (175 Myr). There are two possible scenarios which can account for this situation: (i) If we assume that the differences in the lithium abundances for a given temperatures are no real, that they are an artifact of the chromospheric activity and the presence of inhomogeneities on the stellar surface, as explained above, then we would be comparing stars with the same observed effective temperature, but different masses. The most active star, being also the one with the larger apparent abundance, would be, in fact, more massive. Moreover, the observed lithium equivalent width would not correspond to real one, due to the change of the apparent lithium equivalent width. Unfortunately, no model has been able to quantify properly these effects, in order to remove them and derive real abundances for the Pleiades stars. (ii) An alternative would be the combination of metallicity and the distribution of rotational velocities. As we have shown, M35 has a distribution of rotational velocities much tighter than the Pleiades. Its metallicity is also smaller. If we assume that the distribution of initial angular momentum is tighter in metal-poor stars, the Yale models (Pinsonneault et al. 1990, 1992) would predict a tight dependency of lithium on temperature for M35, compare with the Pleiades.

In any case, the high quality M35 data presented here, together with the rotational velocities and the tight relation between lithium abundance and temperature, makes this young open cluster an ideal laboratory to test theoretical models proposed to explain the lithium depletion in late spectral type stars.

3.5.4. Lithium depletion and age

Figures 8a-f contain several comparisons between M35 probable members and stars belonging to open clusters of different ages. Namely, the

Pleiades, NGC2516, M34, NGC6475, UMaG and the Hyades; with ages 80, 150, 200, 220, 300 and 800 Myr, respectively. Note that other age values can be found in the literature. For the origin of the data and the way they were homogenized, see section 2.2. Temperatures and lithium abundances were derived in the same fashion for all databases. As pointed out by a number of studies (e.g. Balachandran 1995, Pinsonneault 1997; Martín 2000; Jeffries 2000; Deliyannis 2000, and references therein), open clusters of different ages show a characteristic pattern of lithium depletion: the older the age, the smaller the abundance for a given mass. In the particular case of these seven clusters, it is clear that Hyades stars have depleted their lithium in a much larger amount than M35, whereas Pleiades stars (specifically, those of early G spectral type) have kept most of their original content, when M35 stars have already destroyed part of it. NGC2516 data is more sparse, but the data seem to indicate that the distribution of lithium abundances of NGC2516 and M35 stars are alike. Note, however, that NGC2516 shows a spread in the abundances in the Teff range 6000-5000 K not present in the case of M35. Figure 8c seems to indicate that M34 members could have depleted more lithium, on average, than M35 counterpart. However, the lithium spread is quite large in the case of M34 stars. Since the metallicities of both clusters are quite similar, this situation can be interpreted as a sign that M35 is slightly younger than M34 (i.e., younger than 200 Myr). The comparison of the distribution of lithium abundances with clusters in this age range, such as NGC6475, yields similar results: abundances are distributed in similar way, but in this last case, as happens in M35, there is no spread, the relation lithium abundance and effective temperature is quite tight. Again, average abundances of NGC6475 are lower than those characteristic of M35, for a given age. Abundances of UMaG members are more depleted compared with M35 and Hyades members have abundances at least 1.5 dex lower than M35 members.

If we accept that, indeed, M35 is significantly older than the Pleiades, these results fit in the picture, and it is reasonable to assume that the main parameter involved in the lithium depletion is still age (for a given stellar mass). Metallicity, at least in this range of values, is a second order effect. In fact, rotation *per se* could play a secondary

role also in the lithium depletion phenomenon. It is remarkable the fact that between 80 Myr (the Pleiades age) and 175 Myr (our adopted age for the cluster, see section 3.4), the differences between rotation rates for a given mass have disappear and, with them, the lithium abundances have come to the same value (assuming that the Pleiades represents the M35 stage at 80 Myr). We interpret the phenomenon from another perspective. We believe that the Pleiades, in truth, represents the characteristic properties of stars of its age, there is nothing abnormal about the cluster to lead us to think otherwise. However, the differences in abundances for a given mass, the scatter related with rotation/activity might be due to the activity *per se*, at least partially (see the discussion in Section 3.5.3). Therefore, the pattern of lithium depletion in M35 seems to confirm the assumed age of the cluster (\sim 175 Myr) and the effect of rotation and stellar activity on the apparent lithium abundance.

4. Summary and conclusions

We have collected multi-fiber, high resolution spectroscopy of 76 candidate members of the young cluster M35. Our spectra have moderate to high signal-to-noise ratios ($S/N \sim 40-160$), a remarkable feat for stars located at $(m-M)=10.4$. We have measured radial velocities and using these values as membership criterion, we have cataloged 39 stars out of the original 76 as probable members of the cluster. Another 13 stars are spectroscopic binaries and part of them could be members of the cluster. We also have measured rotational velocities via cross-correlation. The comparison between the the rotation pattern of members of M35 and the Pleiades indicates that, indeed, M35 is somewhat older, about 175 Myr, since it lacks fast rotators. Our high quality M35 spectra have been used to derive the metallicity of the brighter and warmer members of the cluster. The result yields $[Fe/H]_{M35} = -0.21 \pm 0.10$, lower than the Pleiades metal content, $[Fe/H] = +0.01$. Subsequently, we have derived lithium abundances of the M35 members, and compared these values with members of other nearby clusters of different ages and metallicities. We conclude that at the age of M35, most of the lithium spread observed in Pleiades stars is not longer present. We have interpreted this fact, at least partially, as an effect of the photo-

spheric spots on the apparent lithium abundance of Pleiades stars. Stellar rotation could also play some role. The data presented in this study are perfectly suited to be used as a validity check of theoretical models involving the lithium depletion.

DBN thanks the “*Instituto de Astrofísica de Canarias*” and “*Ministerio de Educación y Cultura*” (Spain), and the “*Deutsche Forschungsgemeinschaft*” (Germany) for their fellowships. CPD gratefully acknowledges support for this work from the National Science foundation under Grant AST-9812735. JRS acknowledges support from NASA Grant NAGW-2698 and 3690. This work has been partially supported by Spanish “*Plan Nacional del Espacio*”, under grant ESP98-1339-CO2. We appreciate the very useful comments and suggestions by the referee, R.J. García López.

REFERENCES

Anders, E., & Grevesse, N. 1989, in *Geochemica et Cosmochimica Acta* 53:197-214

Balachandran, S. 1995, *ApJ* 446, 203

Barrado, D., Fernández-Figueroa, M. J., Montesinos, B., De Castro, E., Cornide, M., 1994, *A&A* 290, 137

Barrado y Navascués, D., 1996, Ph.D. Thesis, Universidad Complutense de Madrid, Spain

Barrado y Navascués, D., Stauffer, J.R., 1996, *A&A*, 310, 879

Barrado y Navascués, D., 1997, *PASP* 109, 70

Barrado y Navascués, D., Fernández-Figueroa, M.J., García López, R.J., de Castro, E., Cornide, M., 1997a, *A&A* 326, 780

Barrado y Navascués, D., Stauffer, J.R., Hartmann L., Balachandran S., 1997b, *Mem.S.A.It.* 68, 939

Barrado y Navascués, D., de Castro, E., Fernández-Figueroa, M.J., Cornide, M., García López, R.J., 1998, *A&A* 337, 739

Barrado y Navascués, D., 1998, in "10th Cambridge workshop on Cool Stars, Stellar Systems and the Sun", *ASP Conf. Series*, eds. R. A. Donahue and J. A. Bookbinder, p. 894

Barrado y Navascués D., Stauffer, J.R., Bouvier, J., Martín, E.L. 1999, *Ap&SS* 263, 303

Barrado y Navascués D., Stauffer J.R., Patten B.M., 1999, *ApJ Letters* 522, L53

Barrado y Navascués D., Stauffer, J.R., Bouvier, J., Martín, E.L., 2000a, *ApJ*, in press

Barrado y Navascués D., García López, R. Sevérino G., Gomez T., 2000b, *A&A* submitted

Bessell M.S., 1979, *PASP* 91, 589

Bessell M.S., Weis E.W., 1987, *PASP* 99, 642

Boesgaard, A.M., Tripicco M.J., 1986, *ApJ* 302, L49

Boesgaard, A.M., and Budge, K.G., Ramsay M.E., 1988, *ApJ* 327, 389

Boesgaard, A.M., & Friel, E.D., 1990, *ApJ* 351, 467

Butler, R. P., Cohen, R. D., Duncan, D. K., & Marcy, G. W. 1987, *ApJ* 319, L19

Cayrel, R., Cayrel de Strobel, G., & Campbell, B. 1988, *IAU Symp.* 132, *The Impact of Very High S/N Spectroscopy on Stellar Physics*, ed. G. Cayrel de Strobel & M. Spite (Dordrecht: Kluwer), 449

Deliyannis C.P. 1990, Ph.D. Yale University, USA

Deliyannis C.P., Demarque P., Kawaler S.D., 1990, *ApJS*, 73, 21.

Deliyannis C.P., King J.R., Boesgaard A.M., Ryan S.G., 1994, *ApJ* 434, L81

Deliyannis C.P., 2000, in "Stellar Clusters and Associations: Convection, Rotation, and Dynamos". R. Pallavicini, G. Micela and S. Sciortino (eds.) *ASP Conf. Series* 198, 235

Duncan D.K., Jones B.F., 1983, *ApJ* 271, 663

Fernández-Figueroa, M. J., Barrado, D., De Castro, E., Cornide, M., 1993, *A&A* 274, 373

García López, R.J., 1991, PhD Dissertation, Universidad de La Laguna, Spain

García Lopez, R. J., Rebolo, R., Magazzu, A., & Beckmann, J. E. 1991a, *Mem. Soc. Astr. Ital.*, 62, 187

García Lopez, R. J., Rebolo, R., Beckmann, J. E., & Magazzu, A. 1991b in "The Sun and Cool Stars: activity, magnetism, dynamos", I. Tuominen, D. Moss, & G. Rüdiger (eds.), *Lecture Notes in Physics*, Vol. 380, (Berlin: Springer), p. 443

García López, R.J., Rebolo, R., Martín, E.L., 1994, *A&A* 282, 518

Giampapa, M.S., 1984, *ApJ* 277, 235

Gratton R., 2000, in "Stellar Clusters and Associations: Convection, Rotation, and Dynamos". R. Pallavicini, G. Micela and S. Sciortino (eds.) *ASP Conf. Series* 198, 225

Houdebine, E.R., & Doyle, J.G. 1995, *A&A*, 302, 861

James D.J., Jeffries R., D., 1997, MNRAS 292, 177

Jeffries, R.D., Thurston, M.R., Pye, J.P., 1997, MNRAS 287, 350

Jeffries, R.D., James, D.J., Thurston, M.R., 1998, MNRAS 300, 550

Jeffries, R.D., 1999, MNRAS, 309, 189

Jeffries R.D., 2000, in "Stellar Clusters and Associations: Convection, Rotation, and Dynamos". R. Pallavicini, G. Micela and S. Sciortino (eds.) ASP Conf. Series 198, 245

Johnson H.L., Mitchell R.I., 1958, ApJ 128, 31.

Jones, R.B., Shetrone, M., Fisher, D., Soderblom, D.R., 1996, AJ, 112, 186

Jones B. F., Fisher D., Shetrone M., Soderblom D.R. 1997, AJ 114, 352

King J.R., Krishnamurthi A., & Pinsonneault M.H., 2000, AJ 119, 859

King, J. R., Soderblom, D. R., Fischer, D., & Jones, B. F. 2000, ApJ 533, 944

Kurucz R.L., et al. 1984, National Solar Observatory Atlas, vol. 1

Kurucz R.L., 1992, Rev. Mexicana Astron. Astrofis. 23, 181

Leonard P.J.T., Merritt D., 1989, ApJ 339, 195

Martín E.L., Rebolo R., Magazzú A., Pavlenko Ya., 1994, A&A 282, 503

Martín E.L., 1997, Mem.S.A.It. 68, 823

Martín E.L., 2000 in "11th Cambridge workshop on Cool Stars, Stellar Systems and the Sun", ASP Conf. Series, in press.

McNamara, B., Sekiguchi, K., 1986, AJ 91, 557

Mermilliod, J. C. 1981, A&A 97, 235

Mermilliod J.-C., 1996 in "The origins, evolution, and destinies of binary stars in clusters", E.F. Milone and J.-C. Mermilliod (eds.), ASP Conf. Series 90, 475

Mysore S., 1999, PhD. Dissertation, University of Georgia, USA

Parker E.N., 1955, ApJ 122, 293

Pinsonneault M.H., 1997, ARA&A 35, 557

Pinsonneault M.H., Deliyannis D.P., Demarque P., 1991, ApJ 367, 239

Pinsonneault M.H., Kawaler S.D., Demarque P., 1992a, ApJS 74, 501

Pinsonneault M.H., Deliyannis D.P., Demarque P., 1992b, ApJS 78, 179

Rebolo, R., Beckman J.E., 1988, A&A 201, 267

Rebolo, R., 1989, Ap&SS 157, 47

Robichon N., Arenou F., Mermilliod J.-C., Turon C., 1999, A&A 345, 484

Russell, S. C. 1996, ApJ 463, 593

Ryan, S. G., Deliyannis, C. P., 1995, ApJ, 453, 819

Sarrazine, A. R., Steinhauer, A. J. B., Deliyannis, C. P., Sarajedini, A., Bailyn, C. D., Kozhurina-Platais, V., von Hippel, T., & Platais, I., 2000, AAS, 32, #742.

Sneden, C., 1973, PhD Dissertation, University of Texas at Austin, USA

Soderblom D.R., Oey M.S., Johnson D.R.H., Stone, R.P.S., 1990, AJ 99, 595

Soderblom, D.R., Jones, B.F., Balachandran, S., Stauffer, J.R., Duncan, D.K., Fedele, S.B., Hudon, J.D., 1993a, AJ 106, 1059

Soderblom, D.R., Stauffer, J.R., Hudon, J.D., Jones, B.F., 1993b, ApJSS, 85, 315

Soderblom D.R., Pilachowski C.A., Fedele S.B., Jones, B.F., 1993c, AJ, 105, 2299

Sung H., Bessell M.S. 1999, MNRAS 306, 361

Stauffer J.R., 1982, AJ 87 1507

Stauffer J.R., 1984, AJ 280, 189

Stauffer J.R., Hartmann L.W., 1987, AJ 318, 337

Stauffer, J.R., Schultz, G., & Kirkpatrick, J. D. 1998, ApJ, 449, L199

Stauffer J.R., Barrado y Navascués D., Bouvier J., Morrison H.L., Hardig P., Luhman K., Stanke T., McCaughrean M., Terndrup D.M., Allen L., & Assouad P. 1999, ApJ 527, 219

Stauffer J.R., Barrado y Navascués D., 2000, in “11th Cambridge Workshop on Cool Stars, Stellar Systems and the Sun”, ASP Conf, in press

Stout-Batalha N.M., Vogt S.S., 1999, ApJ SS 123, 251

Stuik R., Bruls J.J.M.J., Rutten R.J., 1997, A&A 322, 911

Thorburn, J. A., Hobbs, L. M., Deliyannis, C. P., & Pinsonneault, M. H. 1993, ApJ, 415, 150

Vauclair S., 2000, in “11th Cambridge workshop on Cool Stars, Stellar Systems and the Sun”, APS Conf. Series, in press.

Ventura, P., Zeppieri, A., Mazzitelli, I., & D’Antona, F. 1998, A&A, 331, 1011

Vidal, N.V, 1973, A&ASS. 11, 93

von Hippel, T., Kozhurina-Platais, V., Platais, I., Demarque, P., Sarajedini, A., 2000, in “Clusters and Associations: Convection, Rotation, and Dynamos”. R. Pallavicini, G. Micela and S. Sciortino (eds.) ASP Conf. Series 198, 75

FIGURE CAPTIONS

Fig. 1.— Color-magnitude diagram for M35 candidate members. Note that the reddening $-E(V-I)_c=0.21-$ has not been removed.

Fig. 2.— Spectra of several M35 candidate members observed with WIYN/HYDRA. The top spectrum corresponds to the faintest M35 member in our sample, whereas the bottom spectrum is the brightest. The lithium feature at 6708 Å is easily distinguished.

Fig. 3.— Projected rotational velocity against unreddened $(V-I)_c$ color. M35 probable members as shown as filled symbols (circles for real measurements and triangles for upper limits). **a** Comparison with Pleiades stars (crosses). Values for Pleiades stars derived from $(B-V)$, see text. **b** Comparison with Pleiades stars (crosses). Values for Pleiades stars derived from $(V-I)_k$, see text. **c** Comparison with NGC2516 stars (crosses).

Fig. 4.— Metallicity of the warmest M35 probable members belonging to our sample. Solid and open symbols represent temperatures derived via spectral synthesis and from the photometry, respectively. The solid line represent the average M35 metallicity, whereas the long-dashed line corresponds to the Pleiades.

Fig. 5.— Comparison between the Li I 6708Å equivalent widths of M35 probable members (solid circles) and Pleiades members (crosses, data from Soderblom et al. 1993a) . In panel **a**, Pleiades $(V-I)_c$ data was derived from $(B-V)$, whereas in panel **b** we represent Pleiades $(V-I)_c$ values computed from $(V-I)_k$.

Fig. 6.— Lithium abundances against effective temperatures. M35 probable members are shown as solid circles, whereas Pleiades stars appear as crosses. **a** Soderblom et al. 1993a original data. **b** temperatures and abundances derived from $(V-I)$.

Fig. 7.— Spectra of our coldest targets ($4400 > \text{Teff} > 4200$). Note the effect of rotation and the different strength of lithium feature.

Fig. 8.— Lithium abundances against effective temperatures. M35 probable members are shown

as solid circles (~ 175 Myr). Panels represent several comparisons with data belonging to several open clusters: **a** The Pleiades (70–100 Myr). **b** NGC2516 (120–150 Myr). **c** M34 (200 Myr). **d** NGC6475 (220 Myr). **e** UMa Group (300 Myr). **f** The Hyades (600–800 Myr).

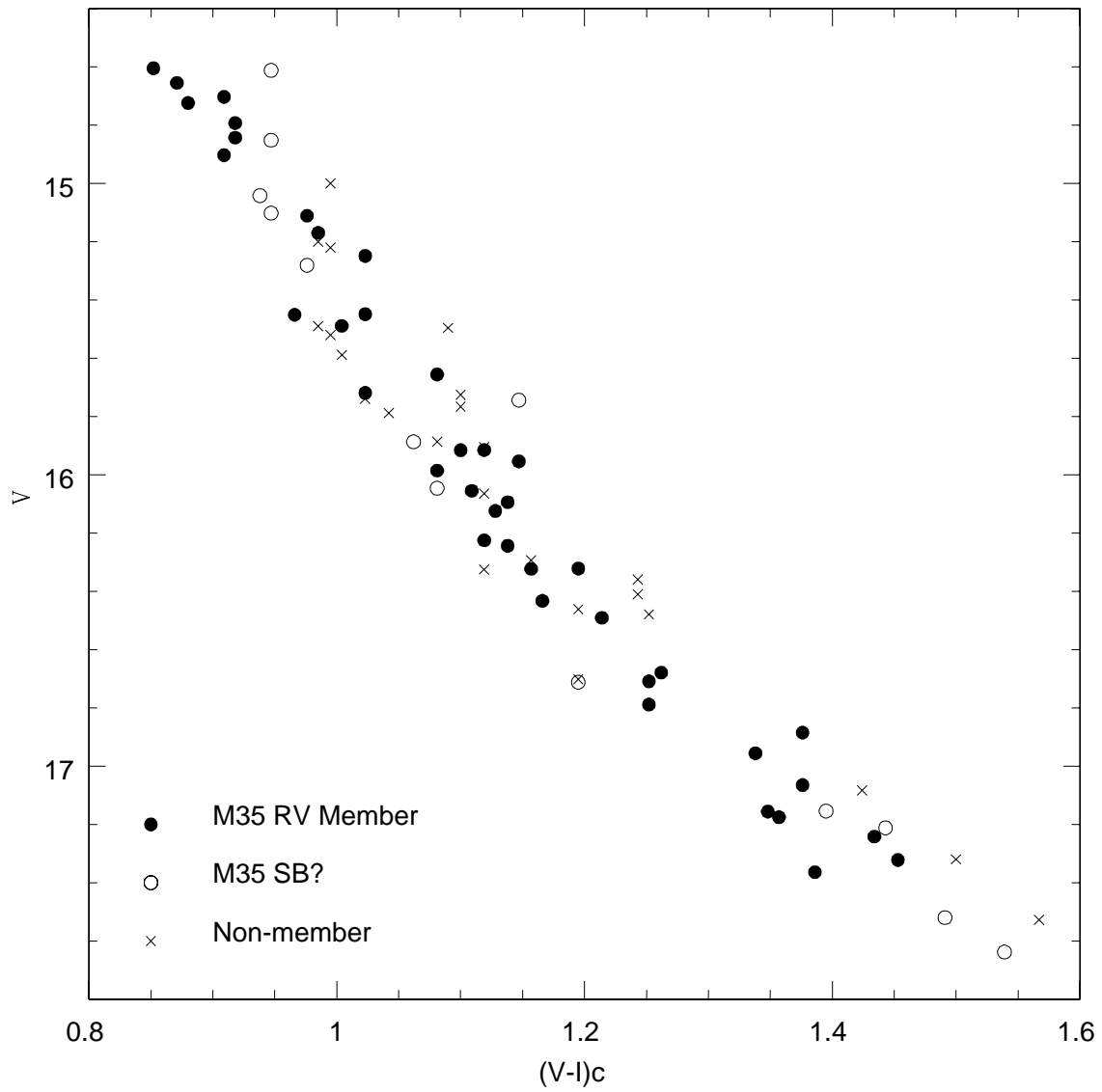


Fig. 1.—

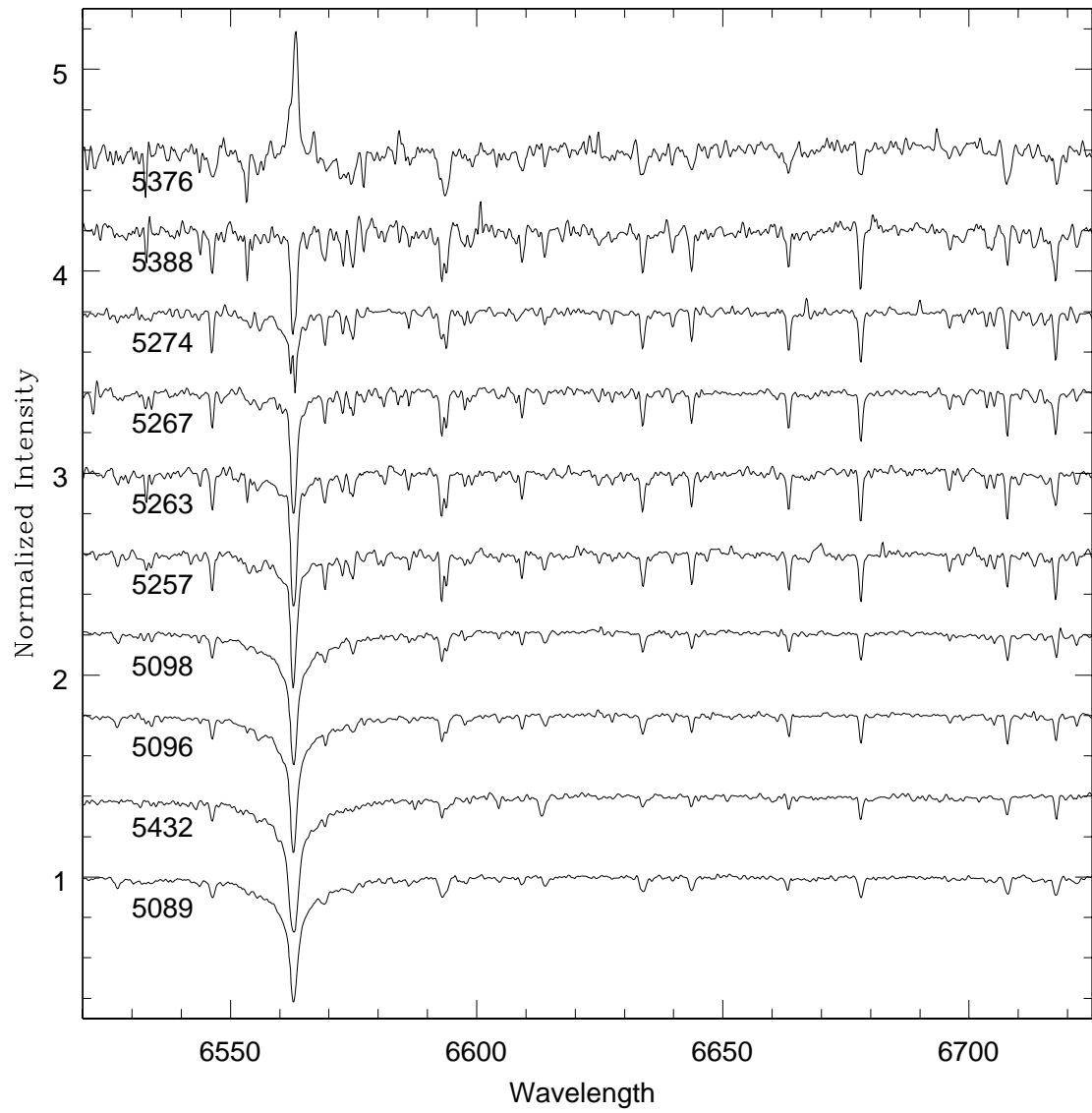


Fig. 2.—

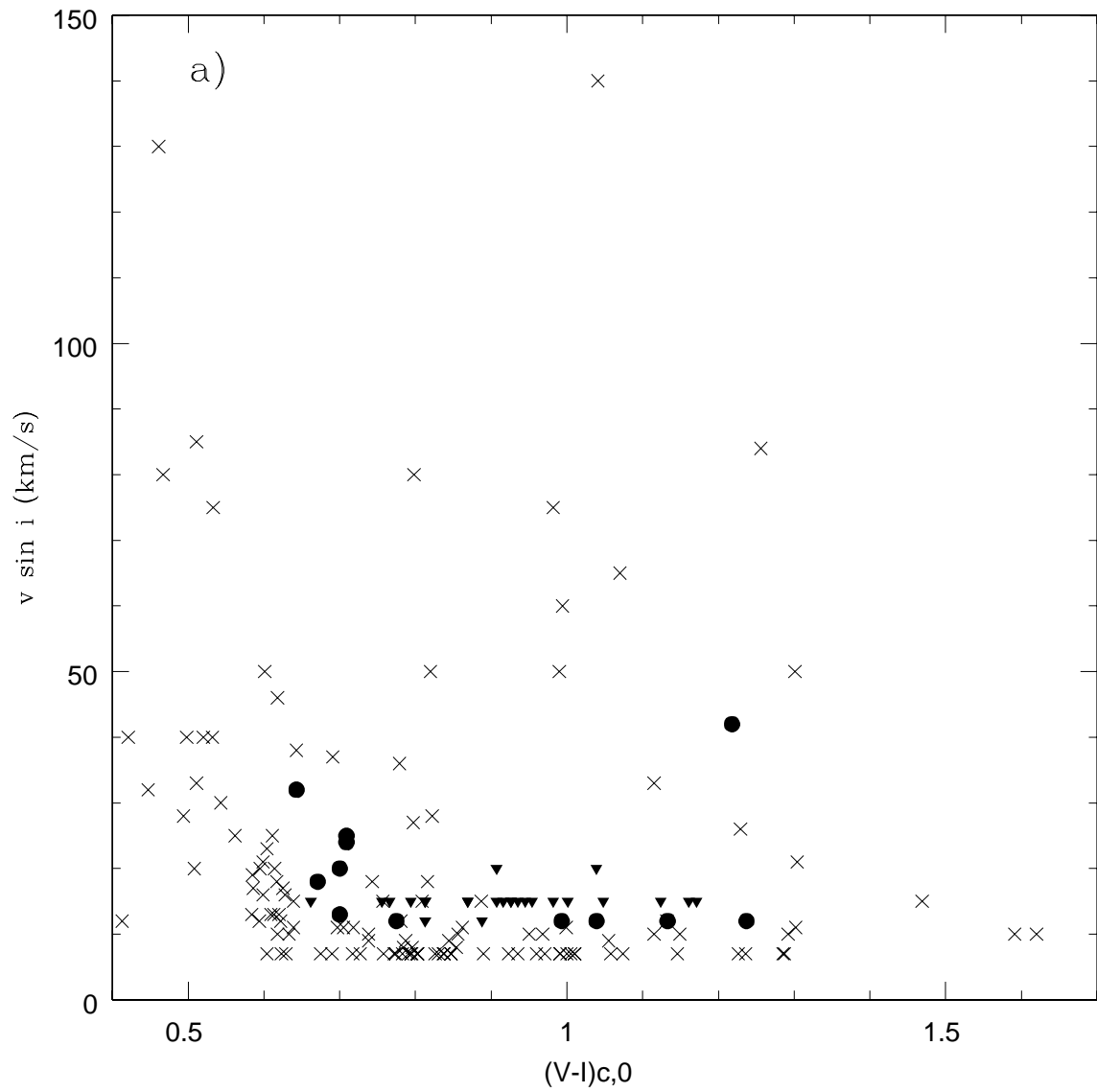


Fig. 3.— a

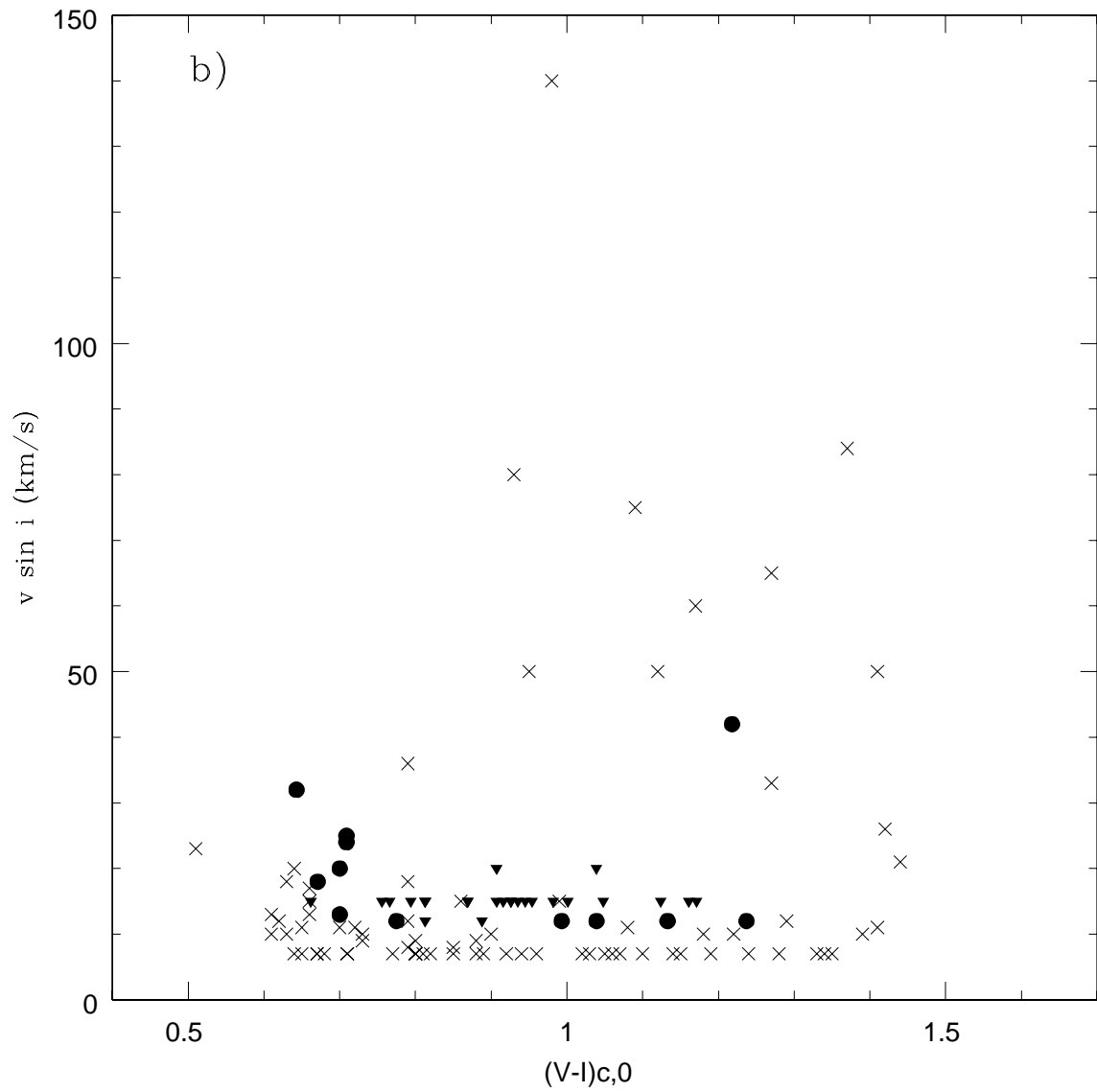


Fig. 3.— b

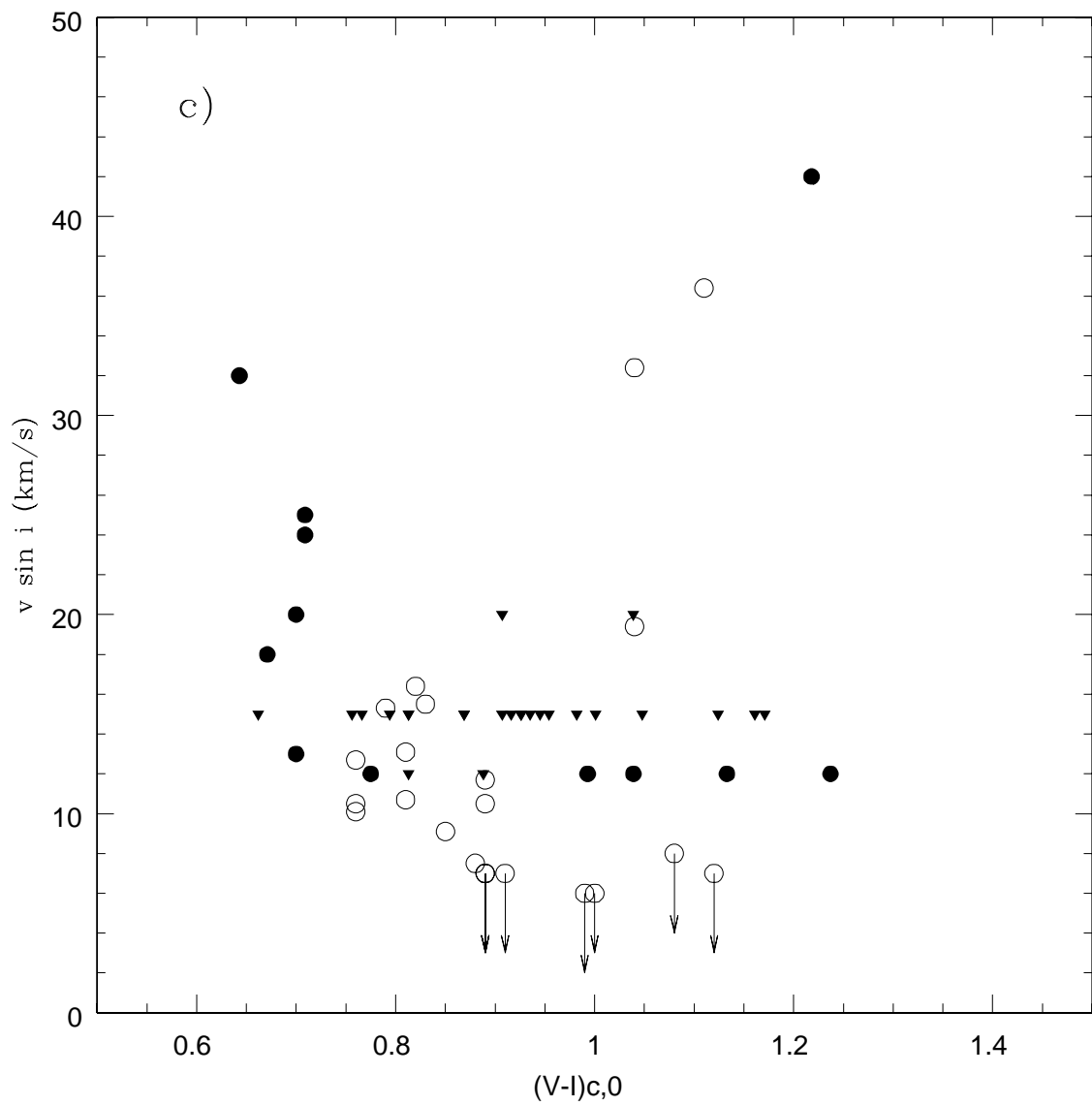


Fig. 3.— c

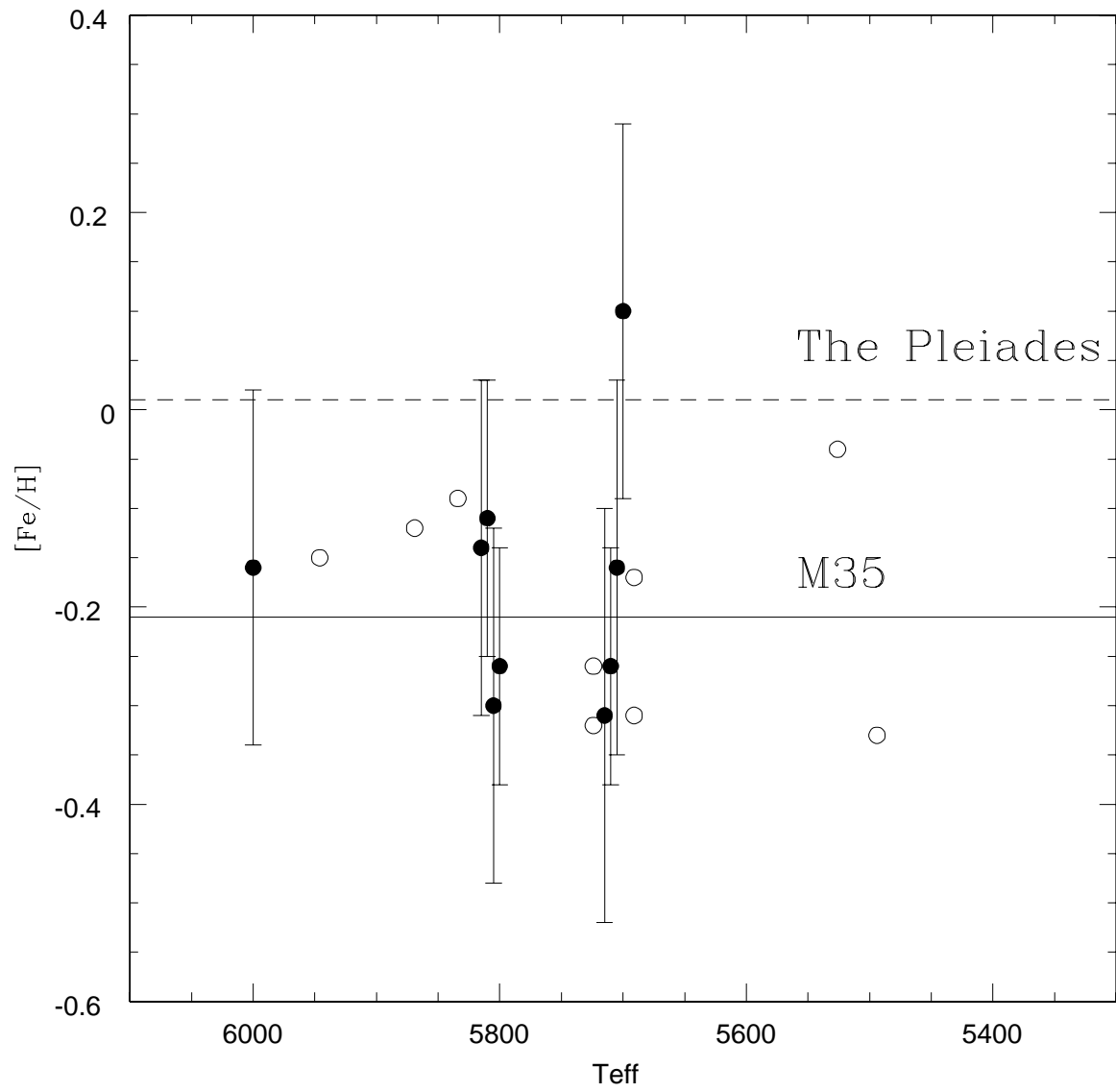


Fig. 4.—

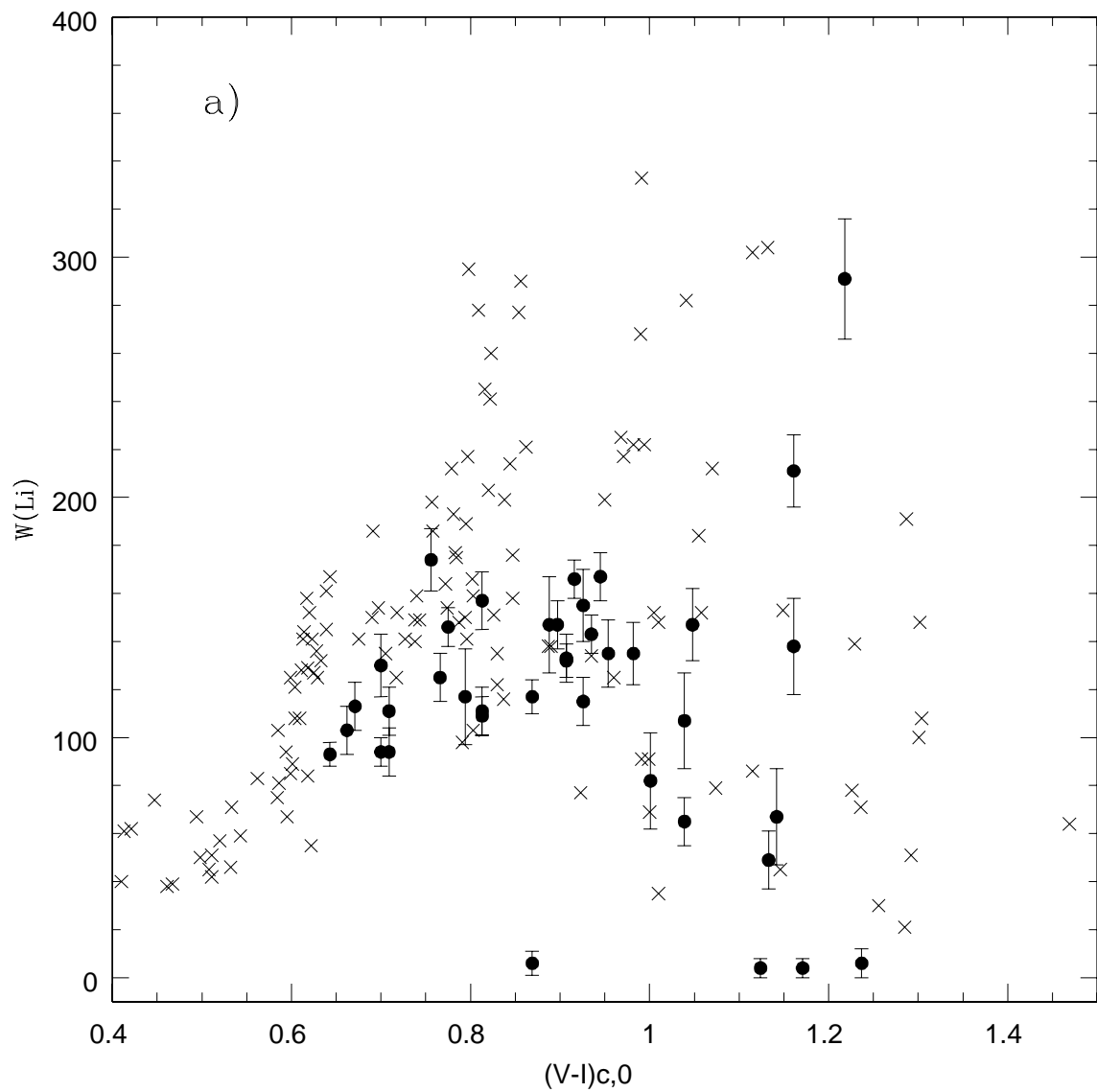


Fig. 5.— a

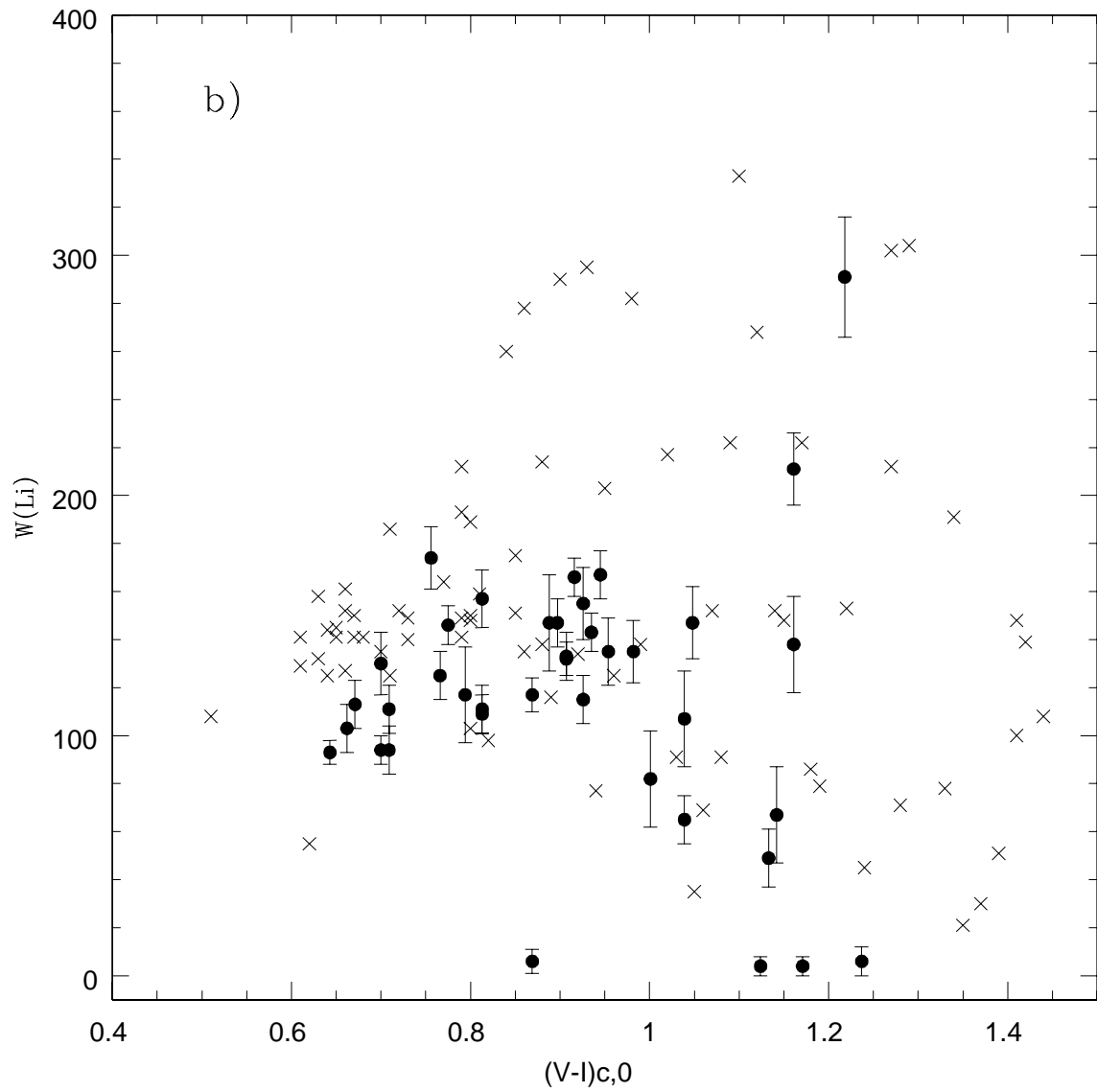


Fig. 5.— b

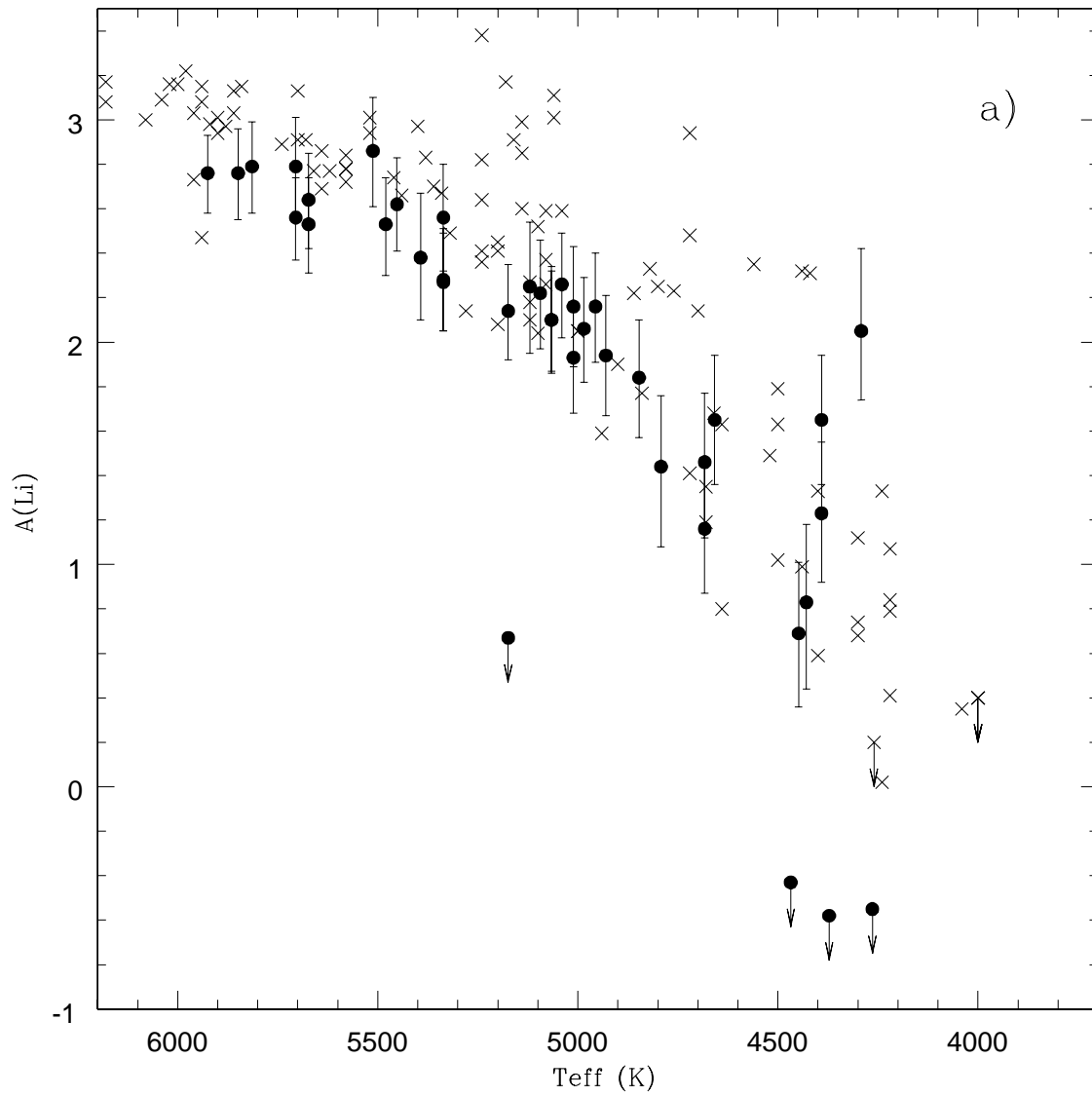


Fig. 6.— a

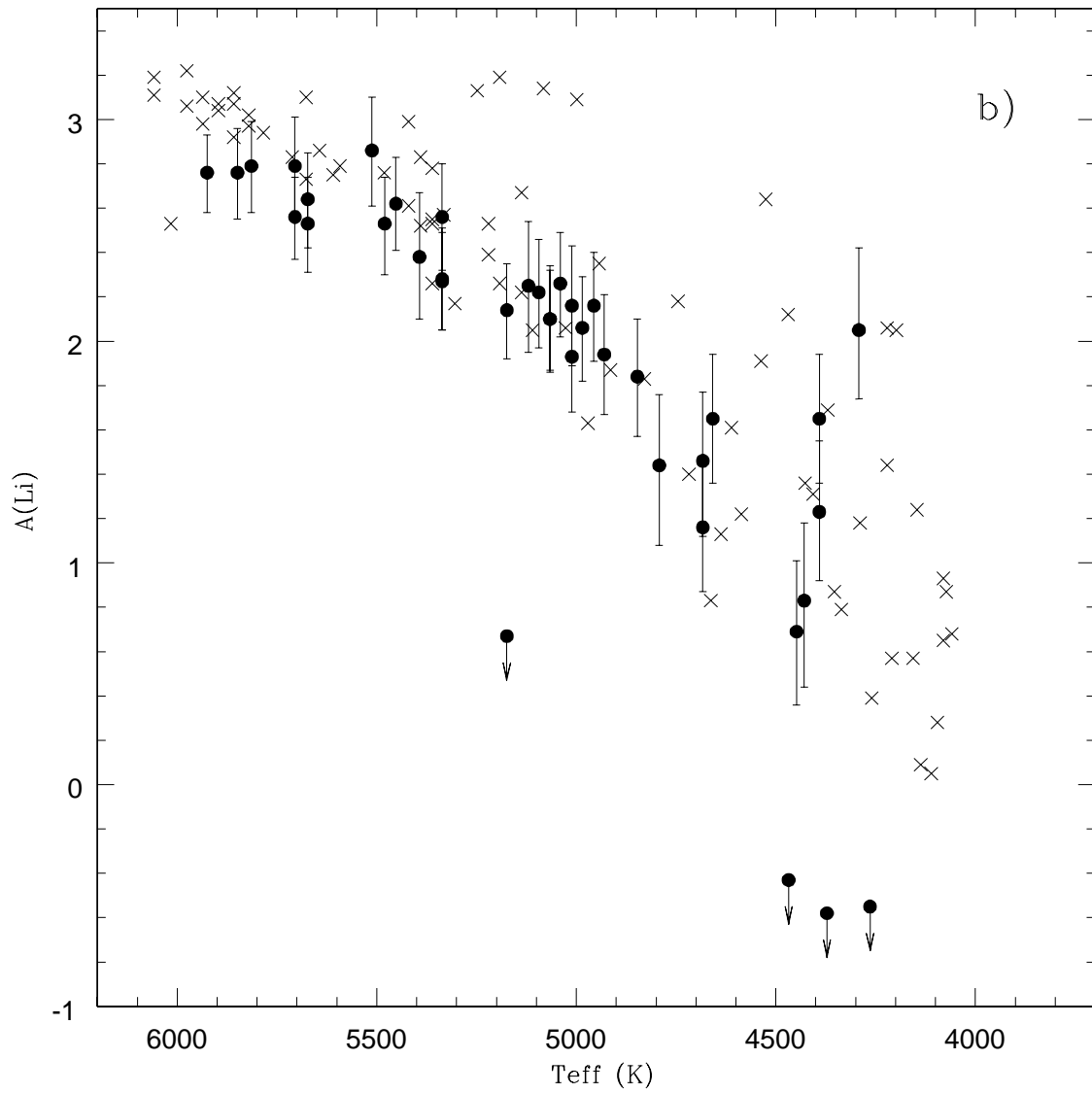


Fig. 6.— b

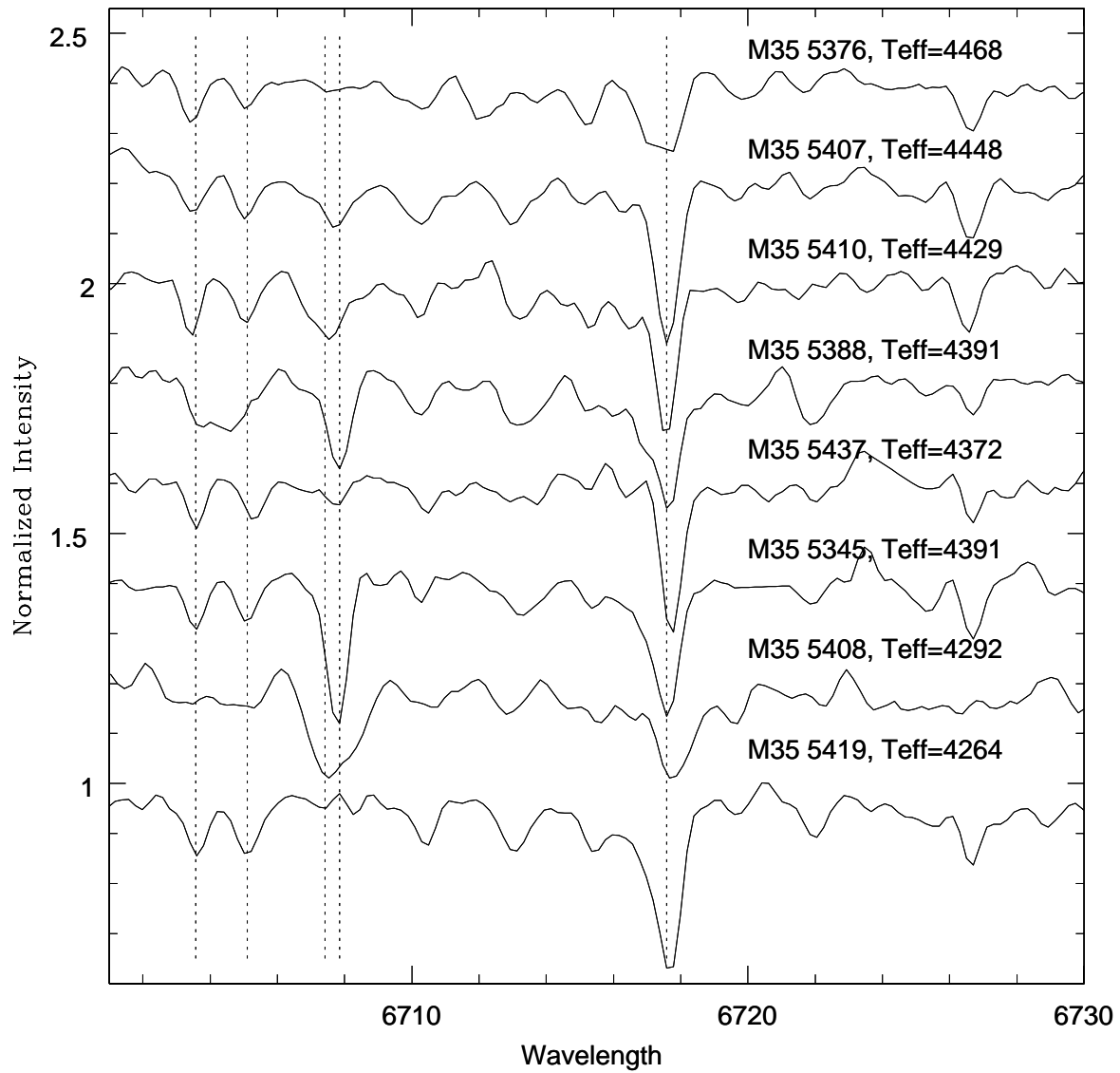


Fig. 7.—

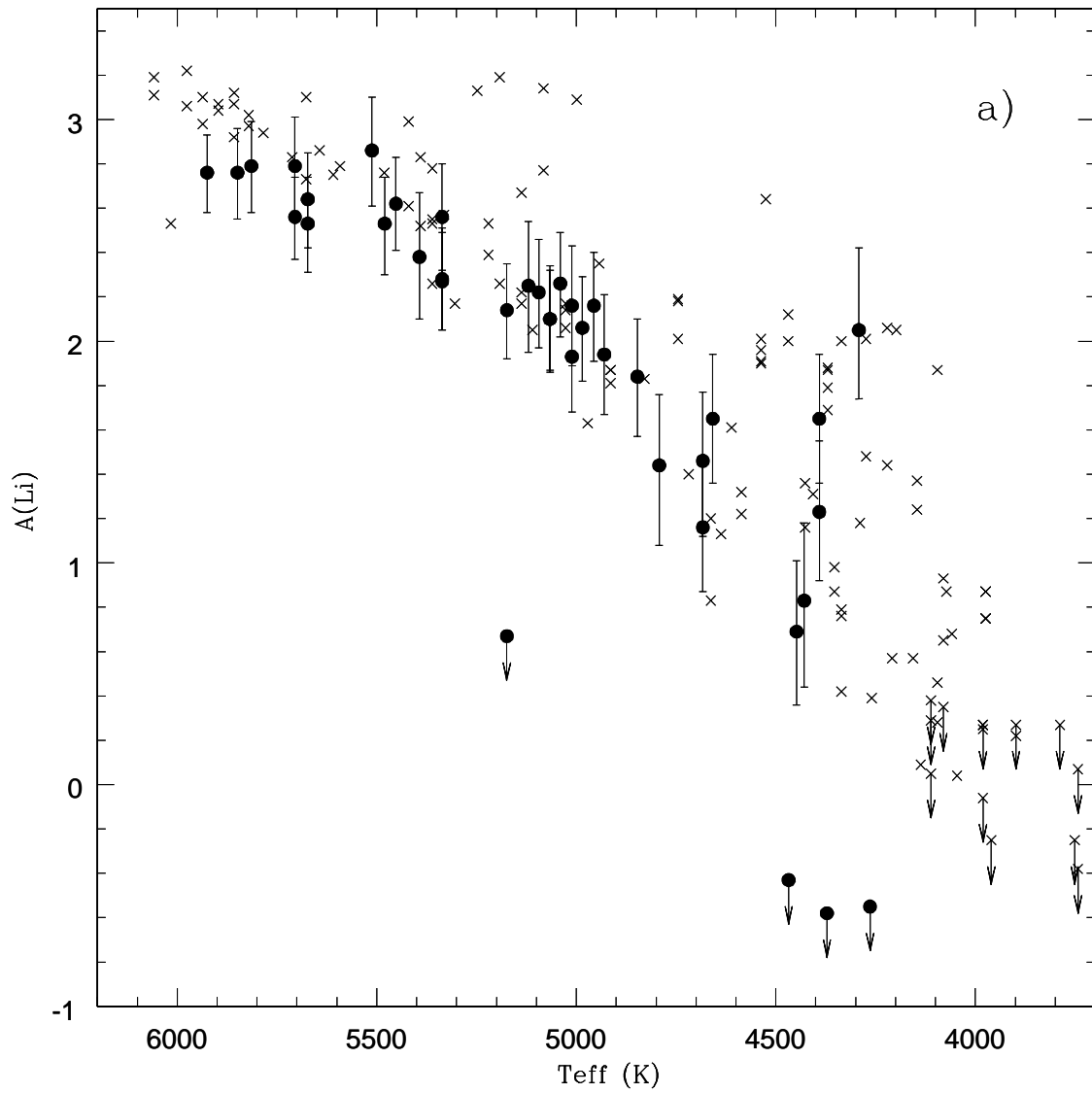


Fig. 8.— a

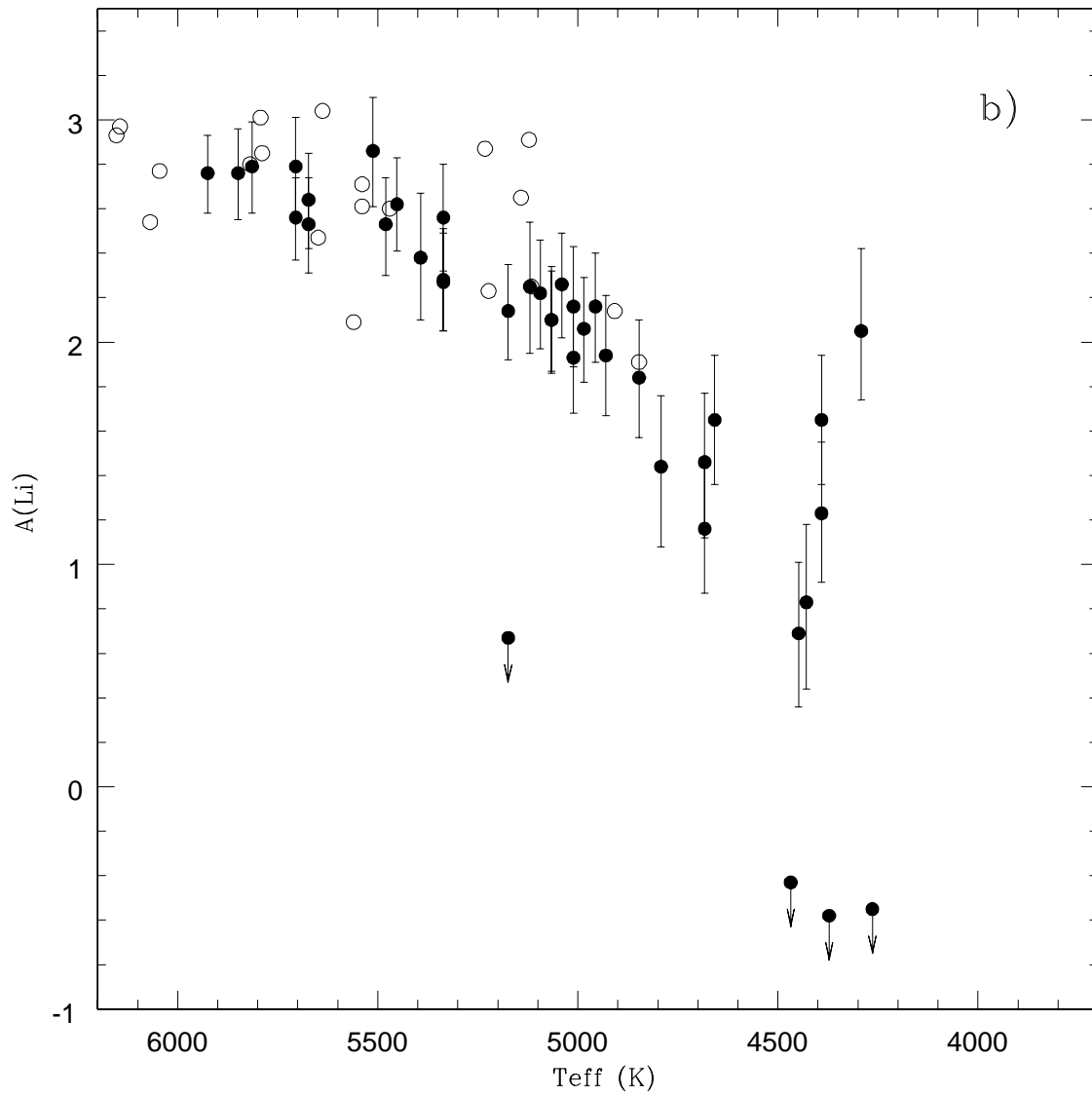


Fig. 8.— b

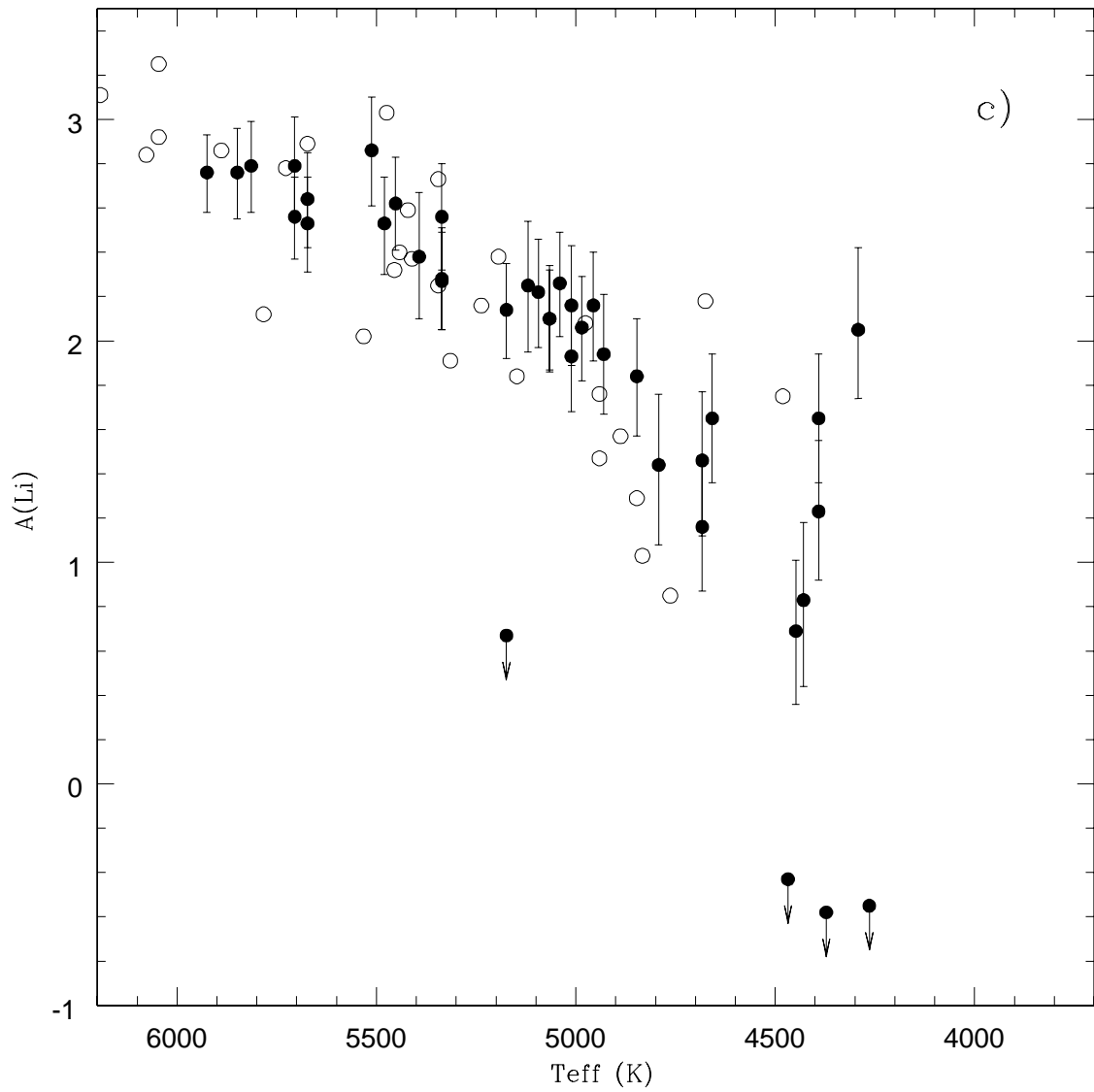


Fig. 8.— c

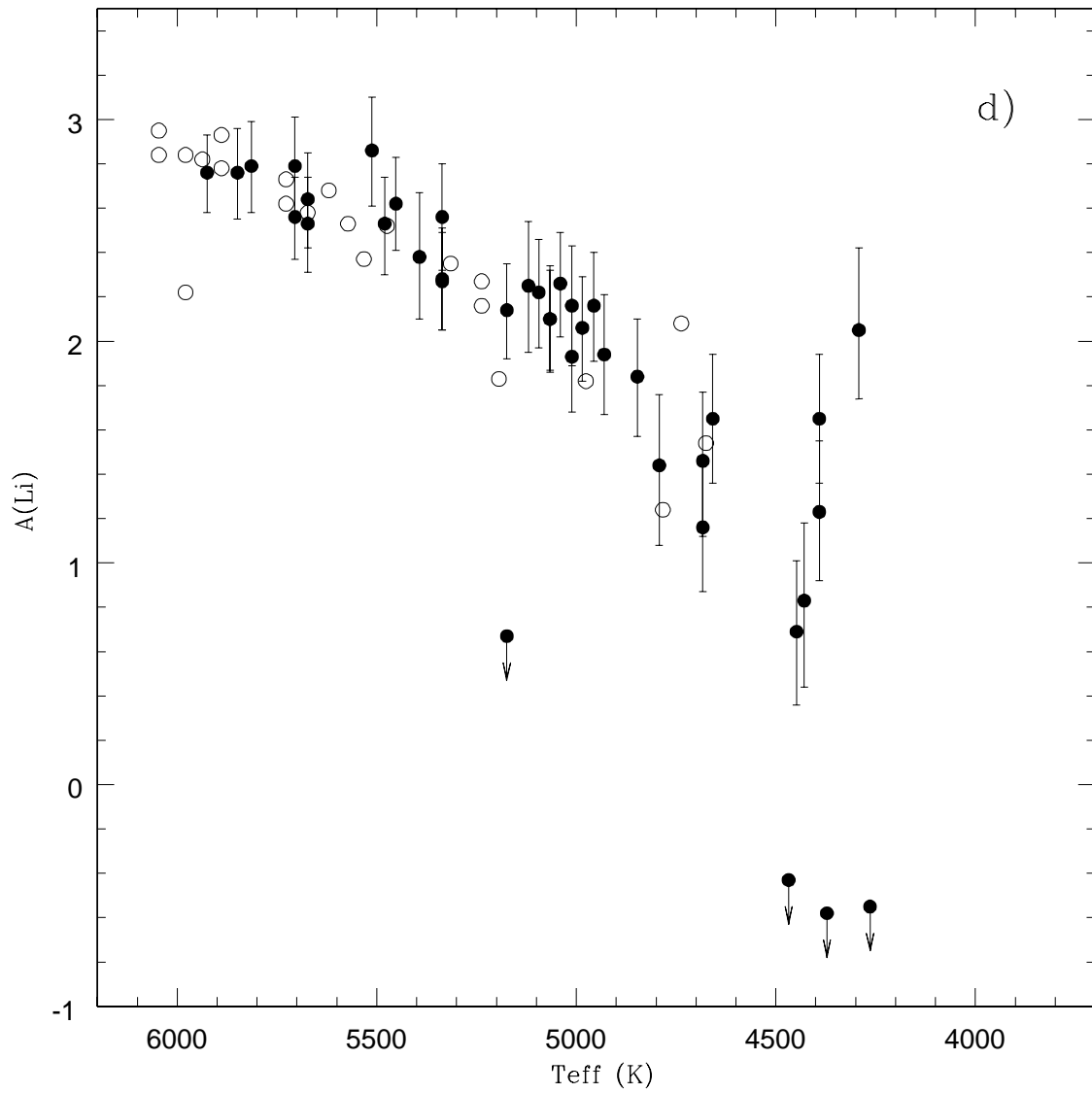


Fig. 8.—d

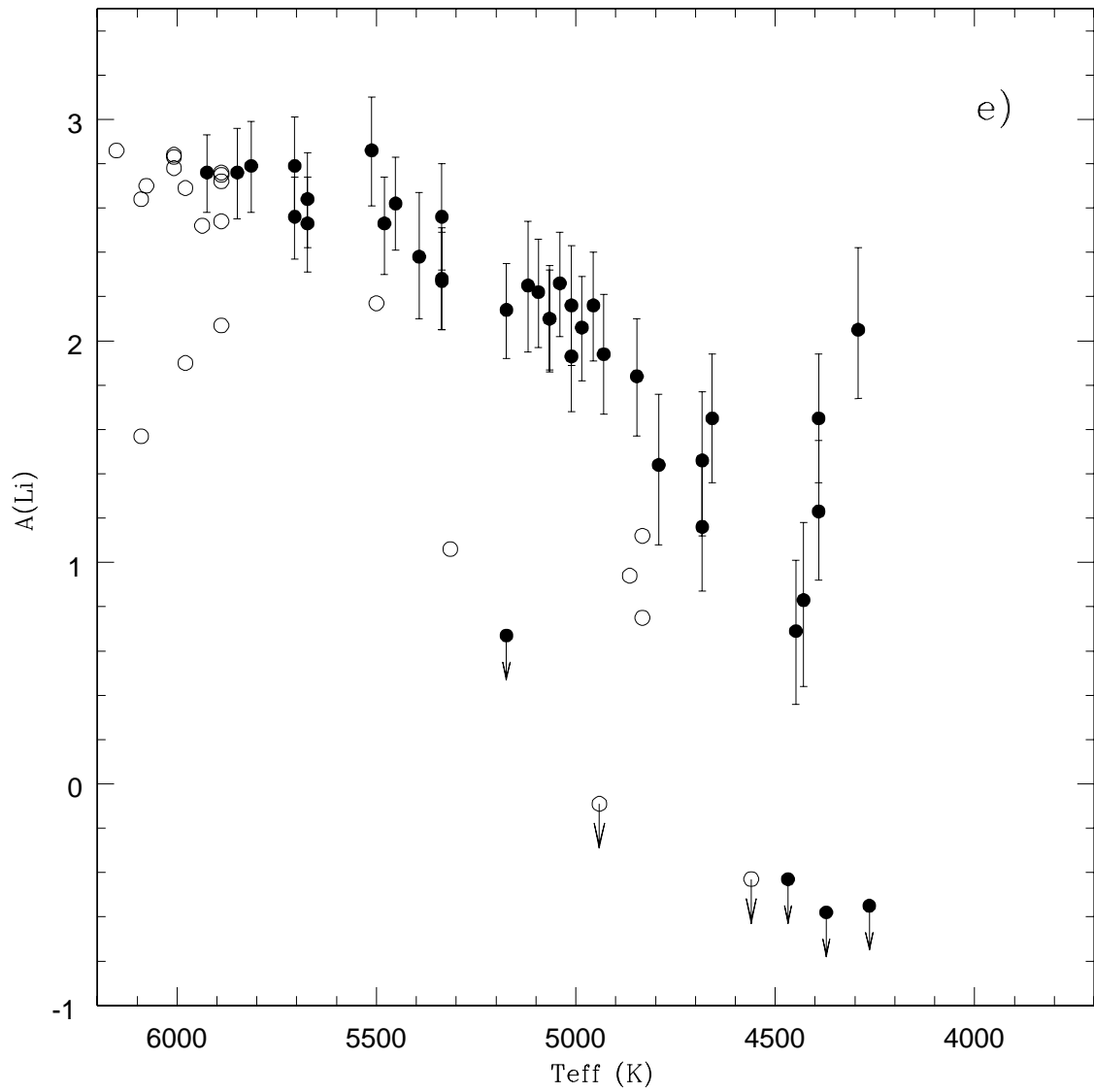


Fig. 8.— e

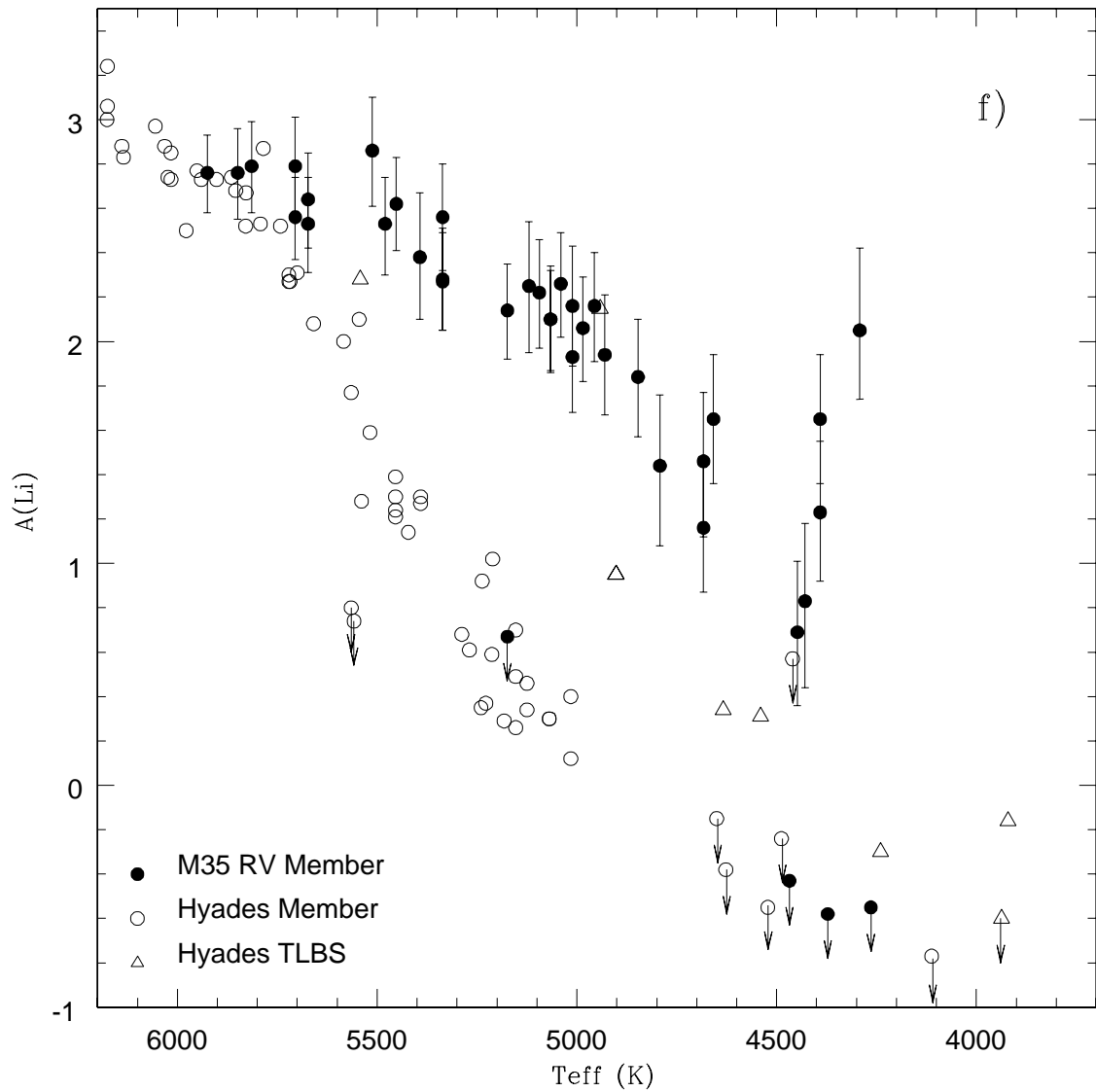


Fig. 8.— f

Table 1: Positions, photometric data and membership status for our M35 candidate members.

ID #	Cuffey/ WEBDA	alpha		delta		V ByN2000	(V-I) _C	V Sung & Bessel (1999)	(V-I) _C	(B-V)	(U-B)	Member?
		(2000.0)										
		(1)	(2)	(3)	(4)	(5)	(6)	(7)	(8)	(9)	(10)	(11)
5081	0691	6:09:26.200		24:29:03.0		14.628	0.951	14.879	1.013	0.768	0.313	SB1
5089	—	6:09:10.230		24:31:44.8		14.622	0.857	—	—	—	—	MEM
5096	1030	6:08:19.030		24:28:37.1		14.672	0.876	14.657	0.872	0.737	0.173	MEM
5098	0178	6:09:26.710		24:18:07.2		14.720	0.914	14.720	0.913	0.751	0.170	MEM
5103	—	6:09:19.600		24:31:57.6		14.741	0.885	—	—	—	—	MEM
5107	0032	6:08:58.860		24:20:17.2		14.809	0.923	14.859	0.936	0.786	0.169	MEM
5113	0405	6:08:47.580		24:12:04.2		14.868	0.951	14.863	0.957	0.787	0.225	SB1
5116	0251	6:08:40.600		24:15:58.4		14.859	0.923	14.877	0.942	0.771	0.199	MEM
5125	3856	6:09:14.810		24:31:23.7		14.920	0.914	15.234	0.984	0.775	0.221	MEM
5126	0704	6:09:36.270		24:27:08.9		15.016	0.998	15.156	1.050	0.857	0.324	NM
5132	0037	6:08:59.070		24:21:00.4		15.058	0.942	15.081	0.985	0.776	0.352	SB2
5135	0128	6:08:52.220		24:23:28.6		15.126	0.980	15.195	1.030	0.831	0.265	MEM
5136	0004	6:09:09.970		24:18:54.5		15.118	0.951	15.141	0.960	0.748	0.307	SB2
5138	3075	6:08:15.410		24:25:27.8		15.186	0.989	15.194	1.003	0.824	0.261	MEM
5141	—	6:08:48.550		24:10:29.0		15.236	0.998	—	—	—	—	NM
5142	—	6:09:43.690		24:21:04.5		15.216	0.989	—	—	—	—	NM
5144	0182	6:09:28.520		24:15:32.1		15.264	1.027	15.327	1.056	0.866	0.347	MEM
5151	0314	6:09:16.980		24:24:19.5		15.296	0.980	15.327	1.021	—	—	SB1
5159	0354	6:09:33.840		24:14:59.9		15.511	1.093	15.525	1.115	0.899	0.309	NM
5165	0383	6:09:15.120		24:11:04.1		15.464	1.027	15.486	1.052	0.846	0.345	MEM
5174	3015	6:08:10.430		24:24:24.7		15.467	0.970	15.452	0.982	0.838	0.334	MEM
5176	3597	6:08:56.400		24:27:10.9		15.505	1.008	15.562	1.027	0.903	0.356	MEM
5178	0048	6:09:10.840		24:19:46.3		15.506	0.989	15.544	1.026	0.811	0.239	NM
5184	0167	6:09:20.740		24:19:55.2		15.536	0.998	15.585	1.051	0.794	0.177	NM
5190	—	6:09:16.060		24:25:31.9		15.671	1.083	—	—	—	—	MEM
5192	0606	6:08:24.170		24:12:23.2		15.605	1.008	15.619	1.006	0.792	0.181	NM
5194	0017	6:09:03.040		24:19:36.8		15.758	1.149	15.768	1.169	0.949	0.422	SB1
5195	3456	6:08:45.830		24:18:23.0		15.740	1.102	15.776	1.141	0.913	0.357	NM
5205	0126	6:08:54.800		24:22:51.1		15.780	1.102	15.811	1.142	1.009	0.548	NM
5209	3088	6:08:17.040		24:27:02.6		15.734	1.027	15.742	1.041	0.919	0.436	MEM
5216	3279	6:08:32.690		24:27:18.9		15.754	1.027	15.756	1.058	0.910	0.385	NM
5219	0289	6:08:47.330		24:24:56.1		15.803	1.046	15.826	1.090	0.999	0.523	NM
5231	3538	6:08:52.710		24:24:44.9		15.920	1.121	15.994	1.182	0.989	0.458	NM
5233	0387	6:09:11.690		24:11:24.5		15.930	1.121	15.942	1.108	0.939	0.542	MEM
5235	0026	6:08:59.030		24:18:25.6		15.968	1.149	16.016	1.172	1.014	0.538	MEM
5236	—	6:09:42.910		24:31:45.0		15.901	1.083	—	—	—	—	NM
5241	0055	6:09:21.840		24:18:22.0		15.930	1.102	15.980	1.128	0.977	0.503	MEM
5243	—	6:09:09.410		24:10:45.7		15.902	1.064	—	—	—	—	SB1
5257	0011	6:09:06.460		24:18:00.3		16.001	1.083	16.048	1.150	1.000	0.495	MEM
5263	3843	6:09:14.070		24:13:37.5		16.070	1.111	16.104	1.137	0.999	0.559	MEM
5264	3751	6:09:07.260		24:23:45.0		16.080	1.121	16.139	1.191	0.985	0.431	NM
5267	—	6:08:57.650		24:10:01.3		16.109	1.140	—	—	—	—	MEM
5268	0333	6:09:26.480		24:20:47.2		16.061	1.083	16.099	1.134	0.849	0.220	SB1
5274	4093	6:09:32.970		24:25:18.5		16.139	1.130	16.215	1.179	1.010	0.678	MEM
5288	4040	6:09:27.930		24:22:27.4		16.259	1.140	16.293	1.207	1.066	0.602	MEM
5289	4050	6:09:29.170		24:21:52.1		16.240	1.121	16.313	1.222	1.040	0.674	MEM
5292	3835	6:09:13.470		24:21:46.8		16.374	1.243	16.444	1.325	1.108	0.622	NM
5293	3743	6:09:06.460		24:21:30.8		16.336	1.196	16.374	1.223	1.051	0.590	MEM
5294	3493	6:08:48.750		24:16:26.6		16.308	1.159	16.343	1.195	0.919	0.216	NM
5297	—	6:08:33.880		24:09:48.4		16.338	1.159	—	—	—	—	MEM
5299	3505	6:08:49.620		24:14:40.1		16.424	1.243	16.480	1.295	1.116	0.944	NM

ID numbers (column 1) and photometry (columns 5 & 6) from Barrado y Navascués et al. (2000b)

WEBDA numbers (Open Cluster database, Mermilliod 1996) coincide with the identification numbers by Cuffey (1938) for the first 778 stars in the WEBDA database.

MEM = Probable Member; NM = Probable non-member; SB = Spectroscopic binary, possible member.

Table 1: Positions, photometric data and membership status for our M35 candidate members (cont.).

ID #	Cuffey/ WEBDA	alpha		delta		V ByN2000	(V-I) _C	V Sung & Bessel (1999)	(V-I) _C	(B-V)	(U-B)	Member?
		(2000.0)										
		(1)	(2)	(3)	(4)	(5)	(6)	(7)	(8)	(9)	(10)	(11)
5305	3365	6:08:39.120		24:24:19.7		16.340	1.121	16.348	1.158	0.956	0.387	NM
5309	–	6:08:06.140		24:27:19.8		16.493	1.253	–	–	–	–	NM
5314	–	6:08:39.200		24:10:45.8		16.476	1.196	–	–	–	–	NM
5316	4024	6:09:26.760		24:27:55.5		16.447	1.168	16.588	1.209	1.064	0.884	MEM
5317	3145	6:08:22.260		24:15:03.3		16.505	1.215	16.521	1.185	1.083	0.772	MEM
5332	3591	6:08:55.970		24:25:11.5		16.693	1.262	16.789	1.348	1.151	0.708	MEM
5339	3880	6:09:16.290		24:18:37.3		16.723	1.253	16.751	1.266	1.138	1.041	MEM
5345	3623	6:08:58.330		24:14:22.2		16.897	1.375	16.851	1.398	1.162	0.782	MEM
5347	3936	6:09:20.340		24:23:05.2		16.716	1.196	16.766	1.241	1.104	0.721	NM
5350	–	6:09:41.770		24:14:59.9		16.726	1.196	–	–	–	–	SB2
5357	3384	6:08:40.610		24:25:40.4		16.803	1.253	16.802	1.294	1.164	0.894	MEM
5376	–	6:09:34.510		24:23:53.9		16.969	1.338	–	–	–	–	MEM
5384	–	6:09:06.130		24:27:20.4		17.095	1.422	–	–	–	–	NM
5388	–	6:08:48.250		24:17:59.8		17.077	1.375	–	–	–	–	MEM
5398	–	6:08:52.550		24:22:00.6		17.166	1.394	–	–	–	–	SB1
5399	–	6:09:12.600		24:22:24.6		17.224	1.441	–	–	–	–	SB1
5407	–	6:09:17.820		24:21:57.1		17.169	1.347	–	–	–	–	MEM
5408	–	6:08:15.230		24:28:06.1		17.254	1.432	–	–	–	–	MEM
5410	–	6:08:23.370		24:23:55.9		17.188	1.356	–	–	–	–	MEM
5411	–	6:08:37.390		24:20:44.0		17.331	1.498	–	–	–	–	NM
5419	–	6:08:43.410		24:20:28.5		17.333	1.451	–	–	–	–	MEM
5432	–	6:09:23.670		24:31:56.3		17.538	1.564	–	–	–	–	NM
5437	–	6:09:23.580		24:26:19.2		17.377	1.385	–	–	–	–	MEM
5449	–	6:09:24.830		24:14:26.5		17.532	1.488	–	–	–	–	SB1
5454	–	6:08:27.400		24:12:08.6		17.649	1.535	–	–	–	–	SB1

ID numbers (column 1) and photometry (columns 5 & 6) from Barrado y Navascués et al. (2000b)

WEBDA numbers (Mermilliod database) coincide with the identification numbers

by Cuffey (1938) for the first 778 stars in the WEBDA database.

MEM = Probable Member; NM = Probable non-member; SB = Spectroscopic binary, possible member.

Table 2: Lithium abundances, radial and rotational velocities for our probable members of M35.

ID	Vhelio (km/s)	W(Li+Fe) (mÅ)	W(Li) (mÅ)	ΔW(Li) (mÅ)	Teff (K)	A(Li)	Teff	A(Li)	ΔA(Li)	vsini (km/s)
							ByN2000		SB1999	
							(6)	(7)	(8)	(11)
5089	-8.2±2.6	102	93	5	5925	2.76	—	—	0.18	32
5096	-6.8±0.2	113	103	10	5849	2.76	5865	2.77	0.21	≤15
5098	-5.0±1.1	104	94	6	5705	2.56	5709	2.56	0.19	13
5103	-9.8±1.6	123	113	10	5814	2.79	—	—	0.21	18
5107	-10.5±1.2	104	94	10	5673	2.53	5627	2.48	0.22	25
5116	-9.3±1.8	121	111	10	5673	2.64	5606	2.57	0.21	24
5125	-7.0±0.8	140	130	13	5705	2.79	5467	2.55	0.23	20
5135	-9.0±0.4	136	125	10	5480	2.53	5327	2.36	0.22	≤15
5138	-9.3±0.8	157	146	8	5452	2.62	5408	2.57	0.21	12
5144	-7.5±1.5	170	157	12	5336	2.56	5251	2.46	0.24	12
5165	-5.2±2.6	124	111	10	5336	2.28	5262	2.20	0.23	≤15
5174	-7.2±0.7	185	174	13	5512	2.86	5474	2.81	0.25	≤15
5176	-3.8±2.2	129	117	20	5393	2.38	5336	2.32	0.29	≤15
5190	-8.6±0.6	23	≤6	5	5174	≤0.67	—	—	—	≤15
5209	-7.3±0.7	122	109	8	5336	2.27	5294	2.23	0.22	≤15
5233	-9.2±0.7	146	132	7	5066	2.10	5103	2.14	0.22	≤15
5235	-9.1±0.7	158	143	8	4985	2.06	4918	1.98	0.23	≤15
5241	-9.4±0.6	161	147	20	5120	2.25	5066	2.18	0.29	≤12
5257	-7.8±0.6	131	117	7	5174	2.14	4982	1.91	0.21	≤15
5263	-8.3±1.5	161	147	10	5094	2.22	5020	2.13	0.25	—
5267	-8.9±0.6	170	155	15	5011	2.16	—	—	0.27	≤15
5274	-8.8±0.8	181	166	8	5040	2.26	4897	2.08	0.24	≤15
5288	-7.8±0.5	130	115	10	5011	1.93	4815	1.68	0.25	≤15
5289	-8.8±0.8	147	133	10	5066	2.10	4772	1.73	0.24	≤20
5293	-8.1±0.8	151	135	13	4847	1.84	4769	1.74	0.26	≤15
5297	-9.2±0.4	182	167	10	4956	2.16	—	—	0.25	≤15
5316	-8.8±0.7	150	135	14	4930	1.94	4809	1.79	0.27	≤15
5317	-6.9±1.2	98	82	20	4792	1.44	4880	1.55	0.34	≤15
5332	-7.8±0.2	165	147	15	4658	1.65	4446	1.36	0.29	≤15
5339	-8.5±0.5	82	65	10	4683	1.16	4647	1.11	0.29	12
5345	-8.5±0.4	230	211	15	4391	1.65	4348	1.59	0.29	≤15
5357	-8.1±1.0	124	107	20	4683	1.46	4573	1.30	0.32	≤20
5376	-10.8±1.0	-99	≤4	4	4468	≤-0.43	—	—	—	≤15
5388	-7.6±1.6	157	138	20	4391	1.23	—	—	0.31	—
5407	-9.3±1.0	68	49	12	4448	0.69	—	—	0.32	12
5408	-7.2±4.1	311	291	25	4292	2.05	—	—	0.34	42
5410	-6.2±1.4	86	67	20	4429	0.83	—	—	0.37	—
5419	-5.7±0.6	18	≤6	6	4264	≤-0.55	—	—	—	12
5437	-6.6±0.7	29	≤4	4	4372	≤-0.58	—	—	—	≤15

SB1999: Values derived using (V-I)c colors from Song & Bessell (1999) .

ByN2000: We used values from Barrado y Navascués et al. (2000b) otherwise.

Table 3: Iron equivalent widths for the brightest members of M35, in mÅ.

FeI $\lambda\lambda$ (Å)	W(FeI) of M35 candidate members, identification numbers								
	#5098	#5103	#5125	#5089	#5107	#5135	#5096	#5116	#5174
6481.870	53	—	—	—	—	—	—	—	—
6569.215	56	96	64	66	66	58	45	64	87
6593.871	78	105	93	—	—	—	—	72	120
6627.545	21	—	—	—	—	—	25	—	45
6677.987	117	186	148	123	132	126	112	153	169
6703.567	21	20	35	19	20	38	28	17	51
6705.103	35	30	38	30	51	40	40	—	74
6710.319	—	11	—	—	—	—	—	—	—
6726.667	—	—	32	—	—	—	38	—	45
6732.065	—	—	—	—	—	4	—	—	—
6733.151	14	—	—	—	26	21	27	9	45
6750.152	74	69	58	72	75	71	51	67	92
6752.707	30	40	—	40	35	39	29	44	48
6810.263	—	36	38	29	49	—	41	42	58
6820.372	24	26	29	19	—	—	—	—	31
6828.591	—	—	—	—	—	—	28	—	—
6837.006	—	—	—	6	—	—	—	—	—

Table 4: Metallicity for the brightest members of M35.

ID # (1)	phot		synthesis	
	Teff (K) (2)	[Fe/H] (3)	Teff (K) (4)	[Fe/H] (5)
5089	5925	-0.15	5805	-0.30 \pm 0.18
5096	5849	-0.12	6000	-0.16 \pm 0.18
5098	5705	-0.32	5800	-0.26 \pm 0.12
5103	5814	-0.09	5705	-0.16 \pm 0.19
5107	5673	-0.17	5810	-0.11 \pm 0.14
5116	5673	-0.31	5715	-0.31 \pm 0.21
5125	5705	-0.26	5710	-0.26 \pm 0.12
5135	5480	-0.33	5815	-0.14 \pm 0.17
5174	5512	-0.04	5700	+0.10 \pm 0.19

We have adopted $\text{Log N(Fe/H)}_{\odot} = 7.52$ dex.